

# The economics of cycling: how a large-scale bike network reshapes local demand

December 23, 2025

## Abstract

Cities are increasingly investing in cycling infrastructure, yet its local economic effects remain poorly understood. We study the effects on brick-and-mortar consumption of the development of a large-scale bicycle infrastructure in Paris (*Plan Vélo*) using geolocated card transaction data by exploiting the variation in market access induced by the new network. Areas experiencing improved access saw a quarterly consumption rise of 4.4%, with larger gains in areas hosting smaller and younger establishments. The new infrastructure also caused a decline in car traffic, while we find no evidence of an impact on business entry or house prices.

Keywords: cities, cycling, infrastructure investment, local economic activity.

JEL Codes: D12, L81, L83, R2, R4

# 1 Introduction

Cities face a fundamental challenge in balancing growth with environmental externalities. As urbanization accelerates globally, dense urban development offers significant potential for reducing per capita carbon emissions through minimized transport needs and optimized energy consumption. However, urban density creates trade-offs; while reducing individual carbon footprints, it can lead to local congestion and higher air pollution ([Carozzi and Roth, 2023](#)). To address these challenges, cities worldwide are stepping up their efforts to promote more sustainable modes of transport, such as developing new cycling infrastructure. Acceptance by local stakeholders is critical for shaping the success of these initiatives. For instance, shop owners may oppose bike lane development because of concerns that reduced car accessibility and parking may harm their businesses<sup>1</sup>. Despite these concerns, empirical evidence on the link between cycling infrastructure and local economic activity remains limited, representing an important knowledge gap in urban environmental policy.

This paper addresses this gap by providing robust evidence of the impact of cycling infrastructure on local economic activity. We study the effects of the development of a large-scale bike lane network on brick-and-mortar consumption as the primary outcome of interest and firm entry, housing prices and car traffic as secondary outcomes. We focus on the deployment of *Plan Vélo* in the city of Paris, a major initiative aimed at promoting a transition towards active mobility that consisted of the construction of approximately 80 km of bike lanes between 2017 and 2020. We leverage the staggered development of the infrastructure and the resulting changes in bicycle travel costs to construct a time and space-varying measure of firm-level potential demand, commonly referred to as market access. Importantly, we allow this metric to account for substitution across different transport modes, which is highly relevant in cities with a significant diversity of commuting habits, such as Paris. We then estimate the elasticity of brick-and-mortar consumption to market access using geolocated data covering nearly the universe of card transactions made by French residents.<sup>2</sup> Using the estimated elasticity, we assess the cumulative gain (or loss) for local businesses and the spatial reallocation of spending.

Market access captures the potential demand each business can reach conditional on consumers' preferred routes and modes of transport. We measure it for every quarter between

---

<sup>1</sup>Various case studies show that retailers overestimate the share of customers that arrive by car and believe that bike lanes might lead to a loss in revenue. See the press article on Bloomberg CityLab "[The Complete Business Case for Converting Street Parking Into bike lanes](#)", accessed on March 16, 2024.

<sup>2</sup>These data were made available thanks to a partnership with *Groupement des Cartes Bancaires CB*, and we exploit the card payments data in accordance with the EU General Data Protection Regulation, in application of Article 89. We use the abbreviation 'CB' hereafter to indicate the source of the card payments.

2015 and 2019 using a 9 arc-seconds grid covering the city of Paris. Market access for a business location is defined as the weighted sum of demand for final goods and services across all possible origin locations for consumers, with weights inversely proportional to the bilateral travel disutility between origin and destination. The development of cycling infrastructure reduces the cost of traveling for given origin and destination pairs, resulting in spatially uneven market access gains. We derive an elasticity of brick-and-mortar consumption to market access by regressing the total value card transactions on this measure. Because variation in our market access measure is driven exclusively by the development of the new cycling infrastructure, the estimated elasticity captures the effect of the new bike lanes on brick-and-mortar consumption.

A potential identification challenge is that the development of bike lanes can be endogenous to the economic activity in a given location. To address this concern, our main specification controls for variation in bike lane availability within the immediate surroundings of each location, which we refer to as *local bike lane density*. The elasticity of interest is thus identified solely from variation in market access generated by bike lane developments occurring farther away, attenuating concerns about the endogeneity of the treatment. This approach relies on a weaker identifying assumption, namely, that the construction of bike lanes in more distant areas of the city is uncorrelated with local economic conditions. Alternatively, we implement an instrumental variable approach that uses changes in market access triggered by the development of distant bike lanes as an instrument for changes in local market access.

Our preferred estimation of the elasticity of brick-and-mortar consumption to market access is 4.5. Using this elasticity, we can calculate that the average improvement in market access, equivalent to the development of 46 meters of bike lanes in a given grid cell, resulted in a 4.4% increase in brick-and-mortar consumption, amounting to approximately 71 thousand euros of higher quarterly spending per grid cell. This effect appears to be driven by an increase in the number of transactions rather than by an increase in the transactions' average value.

Next, we examine whether the new infrastructure affected other key outcomes, namely firm entry, housing prices, and car traffic. We find no statistically significant effect of market access expansion on firm entry. The monopolistic competition model with free entry predicts a positive relationship between market access and firm creation. However, improvements in market access may be capitalized into higher commercial rents, potentially offsetting incentives for potential new entrants. Consistent with this mechanism, we provide suggestive

evidence that an expansion in market access is associated with increases in commercial rents. Second, we find no statistically significant effect of changes in market access on housing prices. In principle, housing prices could respond to the development of new cycling infrastructure through improvements in local amenities (e.g., safer and quieter streets and wider footpaths). However, we argue that our market access metric is best suited to capture the effects of improved connectivity, whereas the measure of *local bike lane density* (the intensity of local bike lane development) serves as a proxy for local amenity improvements. Consistent with this interpretation, and in line with other existing works ([Garcia-López et al., 2024a](#)), we find a positive elasticity of housing prices with respect to local bike lane density. Third, we confirm the critical role played by the development of bicycle infrastructure in achieving positive environmental outcomes. Specifically, we estimate that market access negatively impacts the number of cars transiting through a given grid cell, a proxy for car traffic. This evidence is consistent with a modal shift, where consumers reduce car travel in favor of bicycle travel to locations that witness an increase in connectivity by bicycle. An alternative explanation is that bike lane development occurred along with the removal of car lanes or the introduction of speed limits, which further discouraged car usage.

We implement a large battery of robustness checks to address potential endogeneity concerns. First, we address the potential bias arising from the fact that more centrally located places might be mechanically more affected by infrastructure development ([Borusyak and Hull, 2023](#)). We do so by removing from our sample either “central” locations in a geographical sense, or locations qualifying as transport hubs according to the public transit network. Second, we show the absence of pre-trends in our main outcome of interest, thus minimizing the role of potential biases arising from the endogenous placement of new bike lanes. Similarly, we find no evidence that observable location characteristics systematically predict the timing of bike lane development, thereby ruling out potential biases from endogeneity in network development timing. Third, we show that our results do not change when we consider a smaller, more homogeneous sample of locations. More specifically, we restrict the focus to areas that either witnessed or should have witnessed (but had not, by the end of 2019) the development of some bike lanes according to the original network plan. Fourth, we confirm that our results are not driven by the substitution between card and cash payments.

Next, we investigate the existence of heterogeneous effects by dividing the city into clusters of grid cells, such that the within-cluster business characteristics are sufficiently homogeneous. The positive effect of market access improvement following bike lane development on brick-and-mortar consumption is greater in areas with a higher density of small and young

businesses, as well as food-related businesses, such as cafes, fast food restaurants, and bars. Such heterogeneous effects are consistent with bike lanes attracting more customers to small and newer businesses by increasing salience. Bicycle commuting, with its street-level travel and lower speeds compared to car or public transit, allows consumers to be better aware of shopping opportunities and to take better advantage of them by easily stopping at stores situated along the commuting route. Moreover, pedestrianization infrastructure that often comes along with the development of bike lanes might favor shopping trips that combine cycling and walking, with “footfall” externalities adding to the potential benefits for businesses in areas affected by the new cycling infrastructure (Koster et al., 2019).

Finally, we identify the locations gained or lost in terms of the development of new bicycle infrastructure. We find that market access changes driven by bicycle infrastructure development result in positive pre/post differences in brick-and-mortar consumption for 45% of our sample cells, and negative differences for the remainder. The uneven impact of infrastructure can be explained by analyzing the characteristics of locations that benefited the most from the development of the new bicycle network. These locations tend to be more centrally located and have low residential but high business density. Overall, *Plan Vélo* increased the share of goods and services sold in central districts with lower residential population, at the expense of peripheral areas with higher population densities.

**Related literature** This paper contributes to different bodies of the economic literature. First, it relates to the research strand examining the link between transport infrastructure and economic activity. Earlier studies investigate the impact of accessing new transport infrastructure through a difference-in-difference methodology (Duranton and Turner, 2012; Mayer and Trevien, 2017; Baum-Snow, 2007; Gonzalez-Navarro and Turner, 2018; Garcia-López et al., 2024b; Gibbons and Machin, 2005; Billings, 2011). A more recent set of papers follow a market access approach, in which the potential gains stem from becoming connected to more attractive or richer places as opposed to gaining access to the new infrastructure (Ahlfeldt et al., 2015; Heblich et al., 2020; Gorback, 2022; Tsivanidis, forthcoming; Warnes, 2024).<sup>3</sup> We contribute to this literature by providing the first empirical assessment of the impact of a large-scale cycling infrastructure project on brick-and-mortar consumption of final goods and services in a major European capital. In doing this, we preserve simplicity while

---

<sup>3</sup>A market access-based evaluation has several advantages compared to a simple difference-in-difference setup. First and foremost, a market access approach allows for spatial spillovers by explicitly modeling them, in contrast with a simple difference-in-difference setup. Second, our multi-modal market access metric can account for substitution across modes. Third, a simple difference-in-difference approach cannot distinguish between the effect of improved connectivity and the effect of enhanced amenities brought by the new infrastructure, while with a market access approach, we can separate these two mechanisms.

accounting for the complexity of modal substitution, an important driver of the adoption of transport infrastructure (Beestermöller et al., 2025). To this end, we estimate a multi-modal market access metric that best accounts for substitution across a variety of transport modes available in Paris.

This study is also related to a recent body of literature that focuses on measuring the geography of consumption (of final goods/services) using large-scale spatial datasets, such as online review data (Davis et al., 2019), mobile phone data (Athey et al., 2018; Miyauchi et al., 2021) and card transaction data (Relihan, 2022; Allen et al., 2021; Agarwal et al., 2017; Diamond and Moretti, 2021; Bounie et al., 2023). We contribute to this literature by leveraging a high-frequency, geolocalized card transaction level dataset to measure the effects of new cycling infrastructure on local economic activity covering the near totality of card transactions made by French residents.<sup>4</sup>

We evaluate the economic effects of developing a large-scale cycling network, a policy explicitly aimed at fostering a modal shift towards more sustainable transportation in Paris. Hence, we contribute to the literature on environmental economics, which focuses on the impact of pollution reduction policies in cities, such as car usage restrictions on congestion (Bou Sleiman, 2024; Tassinari, 2024), bike-sharing use (Cornago et al., 2023) and economic activity (Viard and Fu, 2015; Galdon-Sánchez et al., 2023). More closely related to our setting is recent literature evaluating the consequences of cycling infrastructure on bicycle use, car congestion, pollution and housing prices (Hamilton and Wichman, 2018; Thorne, 2022; Bernard, 2023; Garcia-López et al., 2024a).

Our analysis has much in common with Galdon-Sánchez et al. (2023), who examine the impact of car driving restrictions (low emission zones) on local spending in Madrid. They find that areas affected by car driving restrictions experienced a decline in local spending due to reduced accessibility by car. By contrast, we show that improved cycling infrastructure leads to a double gain, by increasing local spending and decreasing car traffic. This difference highlights the benefits of sustainable transport alternatives over car driving restrictions.<sup>5</sup>

The remainder of the paper is organized as follows. Section 2 describes the institutional setting and *Plan Vélo*. Section 3 describes the data used in this study. Section 4 describes the empirical strategy adopted in this paper. Section 5 discusses the results of the analysis. Finally, Section 6 concludes.

---

<sup>4</sup>See Landais et al. (2020) for another application of this data set to study consumption dynamics during the COVID-19 pandemic.

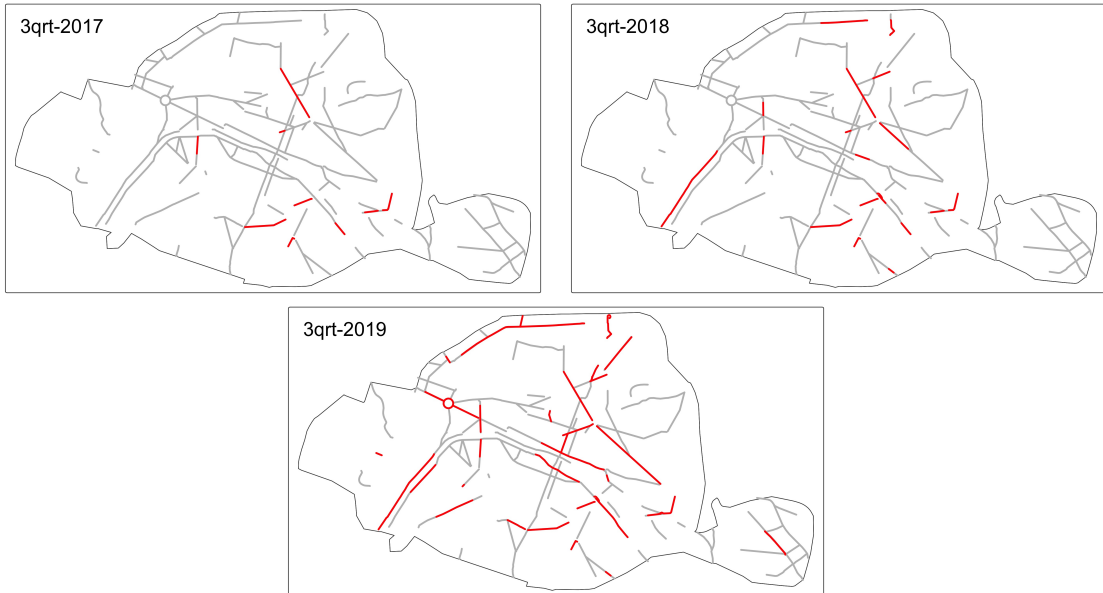
<sup>5</sup>The public intervention under consideration is not the only difference between the two papers. Our paper relies on a market access approach as opposed to a difference-in-difference setup. This has the advantage of allowing us to measure the impact of the intervention broadly across the entire city.

## 2 The *Plan Vélo*

Paris launched an ambitious expansion of its cycling network in 2015 to promote a major shift towards active mobility. The *Plan Vélo* proposed approximately 80 km of new bike lanes for a total investment of 150 million euros (2015–2020). Implementation began slowly, with only 4% of the lanes completed between 2015 and 2017. In February 2017, the independent *Observatoire du Plan Vélo de Paris* was created to monitor progress. Construction then accelerated, with 57 km (71% of the target) delivered between July 2017 and November 2019, the end of our study period. Figure 1 presents the development stages, while bicycle usage increased sharply in parallel, rising at an average monthly rate of 15% over 2018–2019 (Figure A1).

Because the network was coordinated centrally by the municipality, district mayors had a limited influence on the location or timing of construction, reducing concerns about endogenous placement. Instead, timing appears to have followed technical criteria, such as proximity to the two main axes or overall corridor length—supporting our identification strategy, which exploits variation in development status and timing across the city.

Figure 1: Development of *Plan Vélo*



Notes: Red lines show the development of *Plan Vélo* at different points in time; grey lines show the original plan. Source: *Observatoire du Plan Vélo de Paris*.

### 3 Data

The analysis focuses on the municipality of Paris from 2015 to 2019, ending before the COVID-19 shock and is conducted at the quarterly level. We use a uniform grid as the unit of observation, relying on the 9 arc-seconds Global Human Settlement Layer grid ([Schiavina et al., 2019](#)), which divides the city into 2,230 cells (approximately  $270 \times 270$  meters). We exclude cells with more than 75% green space and those without consistent card transaction data over 2015–2019, yielding a final sample of 1,418 cells.

Our main dataset comes from *Groupement des Cartes Bancaires CB* (CB), a consortium covering nearly all French banks that record a large share of consumer expenditures. In 2019, CB captured €494 billion in card payments, about 20% of the French GDP and 60% of household consumption, excluding fixed charges. We use merchant-level monthly data for 2015–2019 reporting transaction value and volume for all payments made with CB cards<sup>6</sup>. Each merchant has a unique identifier, allowing us to link CB data to the national registry to obtain the sector, age, and geographic location.

We retain Paris-based merchants in non-durable brick-and-mortar sectors (retail, restaurants, accommodation, travel agencies, personal services, bakeries, sports clubs, cinemas, theaters), yielding 67,230 establishments that cover 61% of the total card spending in Paris. Our outcomes of interest are total revenue, number of transactions (transaction volume), and average revenue per transaction, aggregated to the grid-cell-quarter level, and log-transformed.

Concerning our secondary outcomes of interest, we begin by measuring business entry using the national business registry. We construct a dummy equal to 1 if at least one entry occurs and 0 otherwise, since most cell-quarter observations contain zero new establishments. Next, we construct a house price index using geolocated microdata on all Paris sales transactions from 2015 to 2019 (*Demandes de valeurs foncières*). After standard cleaning ([Cailly et al., 2019](#)), we estimate a hedonic regression of log prices on housing characteristics with grid-cell and time fixed effects and aggregate predicted prices to the cell-quarter level. Finally, we measure car traffic using publicly available *comptage routier* data from 3,342 sensors across Paris, using 5 p.m. counts averaged at the quarterly level and assigned to grid cells via distance-weighted interpolation.

To construct bilateral travel times by transport mode, we combine data from the *Plan Vélo* infrastructure with OpenStreetMap data and GTFS files for Paris public transit from 2015 to 2019. We build cycling, driving, and walking networks and compute minimum travel

---

<sup>6</sup>In 2019, there were 71 million cards in use in the CB system, and 1.8 million CB-affiliated French merchants ([Groupement des Cartes Bancaires, 2019](#)).

times between grid-cell centroids using Dijkstra's algorithm.<sup>7</sup> Public transit travel times are computed using Conveyal's R5 Routing Engine, which allows for multi-modal trips combining public transit and walking. Using these matrices, we define bilateral travel times  $t_{ijm,t}$  for each origin–destination pair  $(i,j)$ , transport mode  $m$ , and quarter  $t$ . Figure A2 illustrates the evolution of bicycle travel times from *Hôtel de Ville* to all destinations, showing larger reductions in more peripheral districts, where commutes were initially longer and cycling infrastructure sparse.

Finally, we compile time-varying grid-cell socioeconomic and demographic variables using data available from the French National Statistical Institute (INSEE): total population, population aged 25–39, foreign population, number of job seekers, and working-age population. To limit simultaneity concerns, these covariates enter the specification with a three-year lag. INSEE data are provided at the IRIS level (France's census-tract equivalent) and are converted to grid cells using area-overlap weights. Descriptive statistics are provided in Table A1.

## 4 Empirical strategy

The link between the brick-and-mortar consumption of final goods and services and the development of new bicycle infrastructure according to a market access approach can be described as follows:

$$\ln(Y_{it}) = \alpha_i + \alpha_{dt} + \beta \ln(\text{MarketAccess}_{it}) + e_{it} \quad (1)$$

where:

$$\text{MarketAccess}_{it} = \sum_{ij} \frac{\exp(-\hat{\nu}\bar{t}_{ij,t})}{\sum_s \exp(-\hat{\nu}\bar{t}_{sj,t})} \times \text{Population}_j \times \text{Median income}_j \quad (2)$$

In Equation 1, which includes grid cell fixed effects,  $\alpha_i$ , and district×time fixed effects,  $\alpha_{dt}$ , the outcome,  $Y_{it}$ , can be 1) total revenue, 2) transaction volume, and 3) average (per transaction) revenue accumulated across merchants located in grid cell  $i$  at time  $t$ .<sup>8</sup>  $\text{MarketAccess}_{it}$  described in Equation 2 is an empirical proxy of merchant-level market access, capturing the potential demand that merchants located in grid cell  $i$  can reach at time  $t$  conditional on consumers' preferred route and mode of transport. Merchant-level market access is inversely related to estimated expected travel costs,  $\bar{t}_{ij,t}$ , from all consumer locations  $j$ , weighted by

---

<sup>7</sup>See Appendix Section B for details on network construction.

<sup>8</sup>There are 20 districts in the city of Paris, or *arrondissements*.

measured potential spending in those locations,  $\text{Population}_j \times \text{Median income}_j$ , and relative to expected travel costs in other merchant locations  $s$ ,  $\sum_s \exp(-\hat{\nu} \bar{t}_{sj,t})$ , where  $\nu$  identifies the estimated semi-elasticity of bilateral consumption flows to travel costs.

The link between brick-and-mortar consumption and market access can be formalized through a simple partial equilibrium framework, where consumers jointly choose their shopping location and mode of transportation (Appendix C).<sup>9</sup> The development of a new bicycle infrastructure affects the chosen mode of transport to go shopping. Longer commutes are costly, so more people decide to commute by bike when travel times by bike decline. The development of new bicycle infrastructure will also affect the chosen shopping location. An average decline in transport costs cause a shift in expenditure towards locations where the relative decline is larger.

To empirically measure market access in Equation 2, we fix population, median income and travel times by public transport, car and walking to their levels in the first quarter of 2015. Hence, our empirical proxy for market access is allowed to vary exclusively in response to the development of new bicycle infrastructure. Appendix D contains a description of the steps taken to derive the proxy in Equation 2.<sup>10</sup>

Figure 2 shows the change in market access induced by the development of cycling infrastructure. First, market access rises in places situated near a new bike lane if the latter connects with the rest of the network. For example, the construction of bike lanes in the south-west quadrant of the city did not trigger a sizable expansion in market access because these lanes were poorly connected with other parts of the network. Second, market access in given locations increases only if the reduction in bilateral travel costs exceeds the average reduction experienced by other locations.<sup>11</sup>

The potentially non-random placement of transport infrastructure is a challenge when estimating the elasticity of local economic activity to market access. A district government might push the new infrastructure to cross its own neighborhood in order to revitalize it.

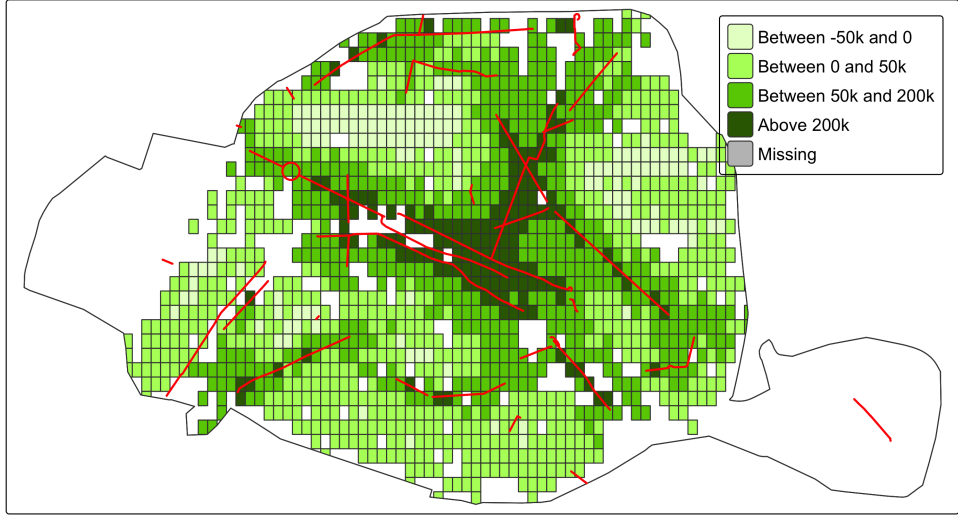
---

<sup>9</sup>While we acknowledge that shopping trips might have other locations as origin, such as the workplace location, our data do not allow us to differentiate revenues depending on trip origin, and thus we assume that shopping trips depart from the home location of consumers. We do not see this as a major limitation of our analysis since non-commuting trips tend to be fairly concentrated around the home location of consumers (Miyauchi et al., 2021).

<sup>10</sup>In synthesis, the empirical market access proxy is obtained by combining observed bilateral travel *times* (Section 3) with the parameters of a modal choice problem estimated via a nested logit specification run on commuting flows data from the 2018 Census (INSEE, 2018). The estimated parameters are used to construct bilateral expected travel *costs*,  $\bar{t}_{ij}$ , and retrieve, together with a subsample of bilateral consumption flows data, the semi-elasticity of bilateral consumption flows to travel costs,  $\nu$ .

<sup>11</sup>Granular bicycle ridership data for Paris are limited, as only 13 of the 32 counters installed between 2018 and 2019 became operational in the fourth quarter of 2019. Nonetheless, available data suggest qualitatively larger increases in bicycle traffic at locations affected by new bike lane developments than at nearby untreated locations

Figure 2: Change in market access between first quarter of 2015 and last quarter of 2019



Notes: Values in nominal euros. Discretized change in absolute terms in market access following the development of *Plan Vélo*, holding the traveling times for the other transport modes constant.

Alternatively, the city administration might choose to target areas that are already growing to provide them with better transport accessibility. The endogeneity of transport infrastructure placement might also stem from the initiative of private interest groups, who might lobby the city or district governments in favor or against implementing the new infrastructure in their neighborhood.

To address these identification concerns, we start by controlling for a set of economic and demographic characteristics ( $X_{it}$ ) varying at the grid cell and time level. The control variables are (log) population, the ratio of foreigners, the unemployment rate and (log) population aged between 25 and 39. Next, we address the remaining identification concerns by letting our coefficient of interest be identified by variation in market access triggered by bike lane development in distant places (Hornbeck and Rotemberg, 2024). This identification strategy requires the inclusion of a *local bike lane density* measure in our specification,  $LBD_{it}$ . By controlling for the intensity of local bike lane development, the market access elasticity is identified by variation in bicycle infrastructure development occurring further away. The identifying assumption is that the construction of bike lanes in more distant areas of the city is uncorrelated with local economic conditions.

With the addition of the just described controls, the baseline estimating equation becomes:

$$\ln(Y_{it}) = \alpha_i + \alpha_{dt} + \beta \ln(\text{MA}_{it}) + \gamma X_{it} + \delta LBD_{it} + e_{it} \quad (3)$$

We test two alternative measures of local bike lane density. Like most infrastructure networks, *Plan Vélo* is articulated into a series of bike lanes (which we refer to as “projects”). In our favorite specification,  $LBLD_{it}$  corresponds to the total length of a given bike lane or project crossing grid cell  $i$  as of time  $t$ . As an alternative measure, we let  $LBLD_{it}$  be equal to the total length of bike lanes situated 1 km around each grid cell  $i$ . This second measure accounts for the fact that development in a given grid cell might be influenced by economic conditions in the immediate neighbors of grid cell  $i$ . We provide a reduced-form test of the relevance of the  $LBLD_{it}$  indicator in Table A2 in the Appendix by regressing total revenue and transaction volumes on  $LBLD_{it}$ . The coefficients of local bike lane density are always positive and statistically significant.

Finally, we run an instrumental variable version of Equation 3, without the local bike lane density control. Market access is instrumented with an alternative definition of the same indicator constructed using bilateral travel times exclusively for locations farther than one kilometer.<sup>12</sup> Alternatively, we also test a different instrument version corresponding to market access constructed excluding origin-destination pairs located along the same bike lane or project.

## 5 Results

### 5.1 Baseline results

Table 1 presents the estimates of  $\beta$  from Equation 3, divided into three panels, one for each outcome: the log of total revenue, the log of transactions volume, and the log of average revenue per transaction. The coefficients of market access are positive and significant for the first two outcomes across all specifications. In column 1, we run Equation 3 without the local bike lane density control (LBD). In columns 2 and 3, we include our two measures of LBD. The instrumental variable results are presented in columns 4 and 5 and are quantitatively similar to the OLS and similarly significant, suggesting that the potential bias caused by the endogeneity in LBD is less of a concern. Conversely, we do not detect a statistically significant elasticity of average revenues per transaction in any of the specifications.

The coefficients of our preferred estimation in column 2 are 4.5 and 3.8 for the total revenue and transaction volume respectively. To interpret them, we rely on the distribution

---

<sup>12</sup>Specifically:

$$MA_{it}^{1km} = \sum_{ij | dist_{ij} > 1km} \frac{\exp(-\bar{\nu}t_{ij,t})}{\sum_s \exp(-\bar{\nu}t_{sj,t})} \text{Population}_j \times \text{Median income}_j$$

Table 1: Elasticity of local economic activity to market access: baseline evidence

<b>Panel A:</b>		Log total revenue				
		(1)	(2)	(3)	(4)	(5)
Log MA		4.054*** (1.070)	4.492*** (1.240)	3.598*** (1.092)	4.394*** (0.95)	4.102*** (1.02)
<b>Panel B:</b>		Log transaction volume				
Log MA		5.025*** (1.098)	3.830*** (1.176)	4.758*** (1.105)	4.741*** (0.98)	4.978*** (1.05)
<b>Panel C:</b>		Log average revenues per transaction				
Log MA		-1.030 (0.810)	0.629 (0.963)	-1.216 (0.802)	-0.404 (0.83)	-0.934 (0.79)
N		27,097	27,097	27,097	27,097	27,097
Controls		X	X	X	X	X
Grid cell FE		X	X	X	X	X
District×Time FE		X	X	X	X	X
LBLD	None	Same project	1km	-	-	
Instrument				1km	Same project	
FS F-stat				3336.68	441167.73	
Estimation		OLS			2SLS	

Notes: Coefficients from the estimation of Equation 3. Standard errors are clustered at the district-time level.

Source: *Observatoire du Plan Vélo de Paris*, INSEE and *Groupement des Cartes Bancaires CB*.

of observed changes in our market access (MA) measure over time. Because our measure of MA allows consumers to travel by different modes (driving, walking, cycling, and public transit), and cycling is the least common modal choice, even relatively sizable decreases in travel times by bicycle will lead to fairly modest increases in our MA measure. In grid cells where MA increased between 2017 and 2019, market access increased on a quarterly basis by 0.93% on average. Hence, the average improvement in MA implies a 4.4% increase in total revenue and a 3.6% increase in transaction volume on a quarterly basis between 2017 and 2019. Using average quarterly revenues per grid cell pre-2017, these average percentage changes translate into an additional 71 thousand euros per grid cell of quarterly revenues and about 1,000 extra transactions in grid cells where MA went up.<sup>13</sup> We provide a more detailed quantification of the impact of infrastructure and its distributional consequences in Section 5.5.

Because our market access metric is microfounded, it depends on a set of assumptions concerning consumer behavior and the economic environment. Market potential, defined as

<sup>13</sup>The back-of-the-envelope calculation is as follows: we obtain 71 thousand euros by multiplying 1.7 million euros (the quarterly revenues of brick-and-mortar stores pre-2017 for the average grid cell) times 0.0093 (the average increase in market access on a quarterly basis between 2017 and 2019) times 4.5 (the estimated coefficient in column 2). We repeat the same steps for the volume of transactions, where the pre-2017 average transaction volume per grid and quarter is around 30 thousand.

$MP_{it} = \sum_{j,j \neq i} \bar{t}_{ij,t}^{-1} \times \text{Population}_j \times \text{Median income}_j$ , is sometimes used in this literature as a reduced-form measure of accessibility that does not rely on model assumptions (Baum-Snow et al., 2020). In Table A3 we report the elasticities based on this metric. The coefficients are larger since market potential features less variation than market access as in Equation 2, but are equally statistically significant.

We find that the positive impact of an improvement in market access on local economic activity materializes with a delay. In Table A4, we replace the baseline measure with its lagged value. We find the elasticity of total revenue to be positive and statistically significant across all lags. Similarly, the elasticity of transaction volume is statistically significant across all lags, and it grows in magnitude as lags of market access further back in time are considered.

Our estimated coefficients primarily measure the impact on economic activity to improved access to transport infrastructure (“connectivity channel”). However, this may not be the only channel at work: the development of a new bike lane might affect positively the revenues of local merchants also through an “amenity channel” by, for example, improving the appearance of the sidewalk or street in which they are located. These two channels are correlated but not entirely collinear. Let us consider, for example, the case of two businesses located in streets where the city council decides to build two spacious bike lanes. Both streets might become cleaner and safer, resulting in more people choosing to shop or eat out in those two businesses through an “amenity” channel. However, if only the first of the two bike lanes ends up connecting with the existing cycling network, then business volume should rise even more for the first business since this is now not only a nicer place to shop, but it has also become a place that is easier to reach. In our setup, the local bike lane density control,  $LBLD_{it}$ , acts as a proxy for the amenity channel. When this variable is added as a control, the remaining variation in market access,  $MA_{it}$ , identifies the connectivity channel.

## 5.2 Other outcomes

In this section, we examine how a set of additional outcomes relates to market access.

**Firm entry** — First, we build a dummy indicator that takes the value 1 when the entry of at least a firm is recorded.<sup>14</sup> An improvement in market access may encourage new firms to enter the market. However, our estimates in column 1 of Table 2 do not support this hypothesis. One potential explanation is the rise in commercial rents. As market access

---

<sup>14</sup>Due to the high frequency and granular dimension of our database, firm entry is very rare, which is why we resort to a dummy indicator.

improves in a given area, the rental rate a prospective business must pay to enter the market also rises, offsetting the benefit from the market expansion. We test this hypothesis in column 4 using data on retail rents from MSCI. Despite data limitations that warrant some caution, the evidence suggests a positive link between market access and retail rents in our setting.<sup>15</sup>

**Residential housing prices** — Next, we investigate whether an improvement in market access affects residential housing prices (see Section 3 for more details on the construction of this variable). An improvement in connectivity should improve the value of properties by making the commute less costly. At the same time, bike lane construction is often accompanied by the introduction of speed limits and the re-making of footpaths to make more room for active mobility, which might increase the value of properties owing to improved amenities.

Our estimated coefficient on market access is not statistically significant (column 2 of Table 2), suggesting a weak and/or slow capitalization of cycling infrastructure improvements in housing prices.<sup>16</sup> However, the coefficient associated with local bike lane density, which proxies more directly for improved amenities, is positive and strongly significant.

**Car traffic** — Car traffic was likely affected by the new infrastructure. As an outcome, we use the log of the total number of cars transiting across a given grid cell during a given time (see Section 3 for more details on the data). An improvement in market access has a negative and statistically significant impact on car traffic (column 3 of Table 2). Multiple mechanisms can explain this result. First, car usage goes down because cycling has become relatively more attractive and a subset of former car users might switch to cycling. Through modal switching, the introduction of bike lanes helps attenuate the negative externalities associated with car congestion, with a positive impact likely extending beyond areas directly affected by the development of bike lanes (Hall, 2021). Second, bike lane deployment typically implies the reduction of street parking and the introduction of speed limits, both of which tend to discourage car usage.

---

<sup>15</sup>MSCI Real Estate Global Intel dataset compiles property-level and fund-level information from contributing investors and managers. The dataset provides annual estimates of market rental values at the neighborhood level (80 neighborhoods in Paris). We assign to each grid cell the rental value of its corresponding neighborhood, or an area-weighted average if it lies across two neighborhoods. The dataset is available for about one-third of grid cells and it has an annual frequency, thus reducing the effective sample to roughly 10% of the original one.

<sup>16</sup>Cycling infrastructure improvements might require longer to be reflected in housing prices. Because our observation window is rather short, we might be unable to detect it.

Table 2: Elasticity of other outcomes to market access

	(1) Business Entry	(2) Log House Prices	(3) Car Volume	(4) Log Retail Rents
Log MA	-0.069 (0.675)	-0.096 (0.274)	-6.159*** (2.038)	10.144* (5.594)
LBLD	-0.001 (0.002)	0.002*** (0.000)	-0.034*** (0.006)	0.004 (0.005)
N	27,097	26,993	26,946	2,540

Notes: Coefficients are estimated from Equation 3 using different outcome variables: an indicator for firm entry (column 1), the log of the housing price index (column 2), the log of car traffic volume (column 3), and average retail rents. Columns 1 and 2 (annual outcomes) include grid cell and year fixed effects, with standard errors clustered at the district-year level. Column 3 includes district-year fixed effects, with standard errors clustered at the same level. Column 4 includes neighborhood fixed effects, with standard errors clustered at the neighborhood-year level. Source: *Observatoire du Plan Vélo de Paris*, INSEE and *Groupement des Cartes Bancaires CB*. Back to Section 5.2.

### 5.3 Robustness

In this section, we conduct robustness tests to address potential concerns that might challenge the causal interpretation of our estimates.

**Centrality bias** — We test the robustness of our results to the exclusion of highly connected districts, which might mechanically benefit more from transport infrastructure development (Borusyak and Hull, 2023).<sup>17</sup> In column 2 of Table 3, we follow Chandra and Thompson (2000) and exclude central districts, specifically *arrondissements* 1 to 4. In column 3, we remove transport hubs. Using information on the public transport network (metro, tramway, and suburban trains),<sup>18</sup> we define as transport hubs those grid cells located less than 500 meters away from stations featuring three or more public transport connections.<sup>19</sup> All coefficients in Table 3 remain positive and statistically significant, alleviating the concern for a centrality bias in our setting. Finally, in columns 4 and 5 we report the coefficients of the long difference version of Equation 3. Here the starting period is the average between the first and second quarter of 2015 and the end period is the average between the third and fourth quarter of 2019. Column 5 adds as a control the log of the distance of each grid cell

<sup>17</sup>The centrality bias test proposed by Borusyak and Hull (2023) is not computationally feasible in our context due to the very granular scope of our analysis. Currently, it takes approximately 7 hours to calculate all travel times by bicycle for every quarter between 2015 and 2019. If we followed Borusyak and Hull (2023) and calculated 999 counterfactual travel time matrices for every quarter between 2015 and 2019, this would take approximately 291 days of computation time.

<sup>18</sup>Data come from *Île-de-France Mobilités* website.

<sup>19</sup>The stations excluded are: Charles-de-Gaulle Étoile, Châtelet les Halles, Cité, Denfert-Rochereau, Gare Montparnasse, Gare Saint-Lazare, Gare de Lyon, Gare de l'Est, Gare du Nord, Haussmann Saint-Lazare/Havre-Caumartin, Invalides, La Motte Picquet - Grenelle, Magenta, Opéra, Place d'Italie, Porte de Choisy, Porte de Vincennes, Porte des Lilas, République, Saint-Michel Notre-Dame, Strasbourg - Saint-Denis.

from the city center (Paris city hall). If central areas receive disproportionate increases in market access due to the intrinsic network structure and the bias increases with proximity to the city center, this specification would partly correct for it (Coşar et al., 2022). In line with the results of the other robustness checks, the coefficients of interest are marginally larger but not significantly different.

Table 3: Robustness tests: dealing with centrality bias

<b>Panel A:</b>		total revenue				
		Log-log			Long difference	
		(1)	(2)	(3)	(4)	(5)
Log MA		4.492*** (1.240)	4.574*** (1.291)	4.604*** (1.242)	9.302*** (2.289)	9.503*** (2.291)

<b>Panel B:</b>		Transactions' volume				
		Log MA			N	
Test	Baseline	Remove central districts	Remove transport hubs	Baseline	Log distance from city center	
Log MA	3.830*** (1.176)	3.953*** (1.218)	3.993*** (1.155)	7.417*** (2.511)	7.507*** (2.515)	
N	27,097	25,197	26,817	1,352	1,352	

Notes: baseline estimation, as in column 2 (col.1) of Table 1; excluding districts 1-4 (col.2); excluding grid cells located within 500 meters of metro or train hubs featuring at least three metro or train connections (col.3). Standard errors are clustered at the grid cell level; long-difference specification:  $\Delta \ln(Y_i) = \alpha_d + \Delta \beta \ln(\text{MA}_i) + \Delta \gamma X_i + \Delta \delta LBLD_i + \epsilon_i$  (col.4); long-difference specification:  $\Delta \ln(Y_i) = \alpha_d + \Delta \beta \ln(\text{MA}_i) + \Delta \gamma X_i + \Delta \delta LBLD_i + \varphi \ln dist_i + \epsilon_i$  (col.5). Source: *Observatoire du Plan Vélo de Paris*, INSEE and *Groupement des Cartes Bancaires CB*.

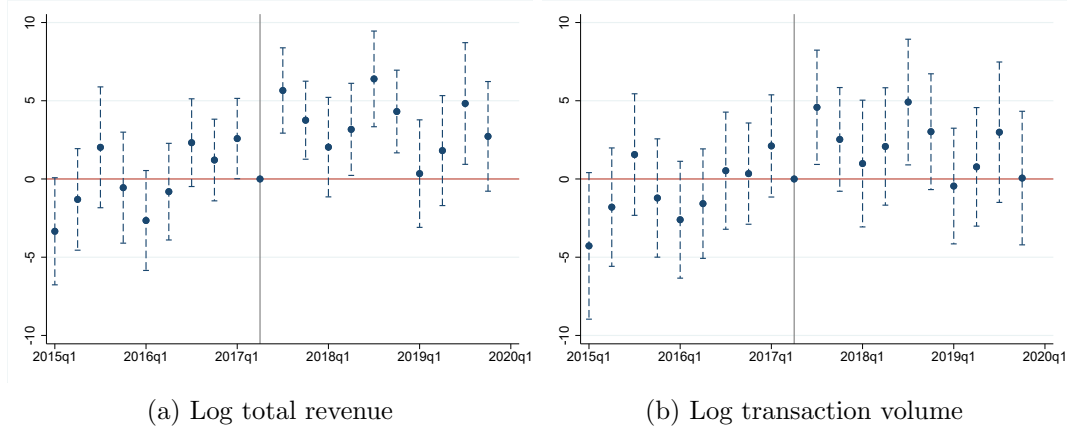
**Non-random bike lane development** — We investigate whether places that experienced a larger increase in market access did not feature a significantly different evolution of the outcome variables before any bike lane development took place. To do so, we run a pre-trends analysis comparing the evolution of the outcome variable in areas with the highest and lowest changes in market access before the development of *Plan Vélo* started. Specifically, we examine whether “most-positively treated” areas—defined as grid cells experiencing the largest increases in market access by the end of the period—were on a different trajectory already before the development started compared to “least-positively treated” areas, which saw the largest declines. To do so, we estimate the following regression:

$$\ln(Y_{it}) = \alpha_i + \alpha_{dt} + \sum_t \beta^t \Delta \ln(MA_{i,15-19}) \times \tau_t + \gamma X_{it} + \delta LBLD_{it} + e_{it} \quad (4)$$

where we regress our outcome variables on the (log) change in market access that occurred during 2015-2019. The (log) change in market access is interacted with time dummies ( $\tau_t$ )

and a full set of time-specific coefficients,  $\beta^t$ , is estimated. If the most-positively treated areas were on a different trajectory compared to the least-positively treated ones already before the start of the development of *Plan Vélo* we would expect the  $\beta^t$  to be positive and statistically significant also for 2015-2017. From Figure 3, we see that places that experienced greater market access improvements featured higher levels of economic activity only after development began, suggesting that non-random bike lane placement does not challenge our strategy.

Figure 3: Pre-trends analysis



Notes: Estimated  $\beta^t$  from Equation 4 on the y-axis. Source: *Observatoire du Plan Vélo de Paris*, INSEE and *Groupement des Cartes Bancaires CB*.

Non-randomness might characterize not only the location of new bike lanes but also the timing of development. Thus, we test whether the timing of the development is as good as random based on observable characteristics (Deshpande and Li, 2019). We take the sample of cells  $i$  such that their treatment status at time  $t = s$  is zero,  $D_{i,s} = 0$ , but which will be eventually developed. Next, we regress the development date of these cells on the set of demographic variables as of  $t = s$  employed as controls in the main specification:

$$\text{Development date}_i | (D_{i,s} = 0) = \alpha + \beta X_{i,s} + e_i \quad (5)$$

We choose three approximately evenly spaced values of  $t = s$  and estimate Equation 5 for these choices. Results are reported in Table A5. During the first months of construction, it appears that places characterized by a lower population, a lower percentage of job seekers and a younger population received access to the bicycle network faster. In the middle of the period (column 2) only the percentage of job seekers seems to matter. Towards the end of our sample period only population appears to be mildly associated with the development date. We interpret the absence of systematic correlation throughout the development period

between the control variables and the development date as indicative of the absence of endogeneity in development timing.

**Exploiting the unfinished *Plan Vélo* —** In a further check, we restrict the sample to cells that should have featured some bike lane development according to the original *Plan Vélo* (see Figure A3). We expect this subsample to be more homogeneous than the baseline sample. We test this hypothesis through a balancing test (Table A7), which confirms that cells that received some bike lane development did not differ in a statistically significant way from cells that did not, except for car traffic, total revenue and the length of planned bike lanes. This last element suggests that the decision to develop first certain bike lanes was partly driven by the need to finish first the long ones, a characteristic likely to be uncorrelated with local economic conditions. We re-run the baseline specification on this subsample and display the results in Table A6. All coefficients remain statistically significant and are slightly larger than in the baseline estimation. The average improvement in market access in this subsample (0.0125) implies an increase in total revenue and transaction volume of 8.8% and 9.9%, respectively.

**Test for card usage —** We test whether the revenue increase in areas with larger market access gains is partly driven by higher card usage rather than overall activity. We examine whether market access is associated with a rise in the share of establishments recording card transactions. For each cell and quarter, we construct a card-usage index by dividing the number of establishments appearing in the CB dataset by the number of establishments expected to be active according to the national business registry. We then re-estimate Equation 3 using this index as the dependent variable. A positive and significant coefficient would indicate that market access improvements increase the share of establishments using card payments, challenging our assumption that card data represent all payments. The insignificant coefficients in Table A8 show that this is not the case.

**Spatial correlation** The highly localized nature of our main variables, both the outcomes and the market access measure, poses challenges for inference, as the assumption of independent and identically distributed (i.i.d.) errors may be violated due to potential spatial autocorrelation. To assess the robustness of our inference, we re-estimate our main specifications using alternative methods for calculating standard errors. In Table A9, columns 1 and 4 report the baseline estimates with standard errors clustered at the district-time level. Columns 2 and 5 present results with clustering at the grid cell level. Finally, columns 3

and 6 feature Conley-adjusted standard errors (Conley, 1999), which explicitly account for spatial and serial correlation in the residuals.

Appendix 7 presents two additional tests addressing household sorting and contemporaneous law contamination.

## 5.4 Heterogeneity

The impact of improvements in market access likely depends on the characteristics of the local urban fabric. Consider, for instance, the examples of: i) a neighborhood characterized by a high incidence of large-scale retailers (e.g., Leroy Merlin, Ikea, Decathlon or large supermarkets), ii) a neighborhood characterized by a disproportionate concentration of shops of well-established luxury brands, and iii) a neighborhood featuring primarily small retailers and a great deal of dining options. In cities, different neighborhoods or, even better, streets tend to have different specializations. In this section, we build clusters of grid cells displaying a similar specialization, or similar establishment characteristics, to explore the potential heterogeneity in the effect of changes in market access. We believe that this approach offers a more flexible solution to the exploration of heterogeneous effects compared to the use of binary indicators, which only allow for the analysis of one heterogeneity dimension at a time.

The characteristics on which we run the clustering algorithm are a set of (dummy-based) sub-industry indicators as of 2015 (supermarkets and malls, specialized food retail stores, specialized non-food retail stores, fast food restaurants and bars, restaurants, bars); a size dummy taking value 1 if in 2015 average merchant size in a given grid cell is greater than the median value; an age dummy taking value 1 if in 2015 average merchant age in a given grid cell is greater than the median value calculated across all cells.<sup>20</sup> Next, we run a *k-means* clustering algorithm (Bock, 2007) for different values of the number of clusters,  $k$ , and we select  $k = 5$  through an elbow test as shown in Figure A5.<sup>21</sup>

The characteristics of the five clusters in terms of the variables used for the clustering exercise are reported in Table A10. The degree of specialization in stores that sell essential goods, such as specialized food retail stores, is fairly homogeneous across clusters, whereas places tend to differ quite substantially in terms of their degree of specialization in fast food, restaurants or bars. Table A11 contains the estimated coefficients from a fully-interacted

---

<sup>20</sup>We define a grid cell as specialized in a given industry if the share of revenues coming from that industry is greater than the share of revenues coming from that industry at the city level.

<sup>21</sup>The elbow method is a heuristic method widely used in data science to determine the optimal number of clusters in a dataset. It consists of plotting the sum of squared errors (SSE) calculated across the identified clusters for each selected number of clusters, and then picking the number of clusters  $k^*$  such that the average reduction in the SSE obtained by moving from  $k_{i-1}$  to  $k_i$  for  $k_i < k^*$  can be considered substantially larger than the one obtained for  $k_i > k^*$ , i.e., by looking for the value of  $k$  corresponding to the elbow of the curve.

version of Equation 3. The evidence suggests a positive and statistically significant impact of a market access improvement on economic activity for grid cells specialized in smaller and younger establishments or fast-foods, cafes, and bars. In contrast, clusters specialized in retail and older businesses do not seem to be as sensitive to changes in market access. A potential explanation is that the development of new cycling infrastructure helps improve establishments' salience, particularly for younger, smaller and thus less known businesses. People switching from public transport (most notably underground) to cycling start commuting on the surface and can more easily become aware of available shopping opportunities. These, in turn, become easier to exploit thanks to the greater ease with which one can stop and park her bike (compare, for instance, to cars).

## 5.5 Distributional consequences of *Plan Vélo*

New infrastructure entailed potentially significant spatial reallocation of consumption. The approach taken in this paper is suited to analyze the distributional consequences of the new infrastructure, while it lacks the features necessary to analyze the absolute gains. Market access in a given place increases if bilateral travel costs to that place decline, on average, more than to other places in the city. Essentially, this means that market access gains in a given place can take place only at the expense of other locations.

Our framework enables us to identify what are the places that have gained in relative terms and those that lost with the development of the new infrastructure. We multiply the difference between the last quarter of 2019 and pre-*Plan Vélo* market access by 4.5 (the baseline elasticity - see column 2 of Table 1), thus obtaining the percentage point change in total revenue implied by the development of *Plan Vélo* only. We find this difference to be positive for 45% of cells (4.1 p.p. on average across “winners”) and negative for 55% (−2.2 p.p. on average across “losers”).

The uneven impact of the infrastructure can be best explored through the examination of which areas gained from the development of the new infrastructure and which areas lost. Figure 2 shows that improvements in market access have been concentrated in more central locations. Improved cycling connections reduced the cost of traveling from the center to peripheral neighborhoods and vice versa. The gains, however, mostly accrued to businesses located in the city center who could count on an increase in demand from peripheral neighborhoods, where on average total income is higher, primarily due to higher population levels (Figure A4).

## 6 Conclusion

Despite many existing narrative accounts, sound quantitative assessments of the consequences of bicycle infrastructure development on local economic activity are scarce. The development of bicycle infrastructure can affect local economic activity in different ways. It can reshape the geography of spending towards locations that become more accessible. Furthermore, they can benefit certain local businesses by making them more salient and easier to visit.

We evaluate the impact of Paris's *Plan Vélo* bicycle infrastructure program (2017–2019) on brick-and-mortar consumption using card transaction data. We find robust evidence that increased market access from the new infrastructure boosted economic activity in affected areas.

When assessing additional relevant outcomes, we find that *Plan Vélo* produced a significant reduction in car traffic in areas where accessibility by bicycle improved the most. This is especially relevant given the stated goals of promoting a transition towards more sustainable transportation and a reduction in traffic-related emissions.

Our analysis of the distributional impact of the new infrastructure highlights how *Plan Vélo* redistributed economic activity away from more peripheral districts that are more densely populated towards more centrally located ones. These results confirm the importance of considering the distributional effects when designing place-based environmental policies.

## References

- AGARWAL, S., J. B. JENSEN, AND F. MONTE (2017): “Consumer mobility and the local structure of consumption industries,” Tech. rep., National Bureau of Economic Research.
- AHLFELDT, G. M., S. J. REDDING, D. M. STURM, AND N. WOLF (2015): “The economics of density: Evidence from the Berlin Wall,” *Econometrica*, 83, 2127–2189.
- ALLEN, T., S. FUCHS, S. GANAPATI, A. GRAZIANO, R. MADERA, AND J. MONTORIOL-GARRIGA (2021): “Urban Welfare: Tourism in Barcelona,” .
- ATHEY, S., D. BLEI, R. DONNELLY, F. RUIZ, AND T. SCHMIDT (2018): “Estimating heterogeneous consumer preferences for restaurants and travel time using mobile location data,” in *AEA Papers and Proceedings*, vol. 108, 64–67.
- BAUM-SNOW, N. (2007): “Did Highways Cause Suburbanization?” *The Quarterly Journal of Economics*, 122, 775—805.
- BAUM-SNOW, N., J. V. HENDERSON, M. A. TURNER, Q. ZHANG, AND L. BRANDT (2020): “Does investment in national highways help or hurt hinterland city growth?” *Journal of Urban Economics*, 115, 103124.
- BEESTERMÖLLER, M., L. JESSEN-THIESEN, AND A. SANDKAMP (2025): “Striking evidence: the impact of railway strikes on competition from intercity bus services in Germany,” *Journal of Economic Geography*, 25, 853–872.
- BERNARD, L. (2023): “The impact of segregated cycling lanes on road users,” Available at SSRN 4353625.
- BILLINGS, S. B. (2011): “Estimating the value of a new transit option,” *Regional Science and Urban Economics*, 41, 525–536.
- BOCK, H.-H. (2007): “Clustering Methods: A History of k-Means Algorithms,” In: Brito, P., Cucumel, G., Bertrand, P., de Carvalho, F. (eds) *Selected Contributions in Data Analysis and Classification. Studies in Classification, Data Analysis, and Knowledge Organization*.
- BORUSYAK, K. AND P. HULL (2023): “Nonrandom exposure to exogenous shocks,” *Econometrica*, 91, 2155–2185.
- BOU SLEIMAN, L. (2024): “Are car-free centers detrimental to the periphery? Evidence from the pedestrianization of the Parisian riverbank,” Working paper.
- BOUNIE, D., Y. CAMARA, AND J. W. GALBRAITH (2023): “Consumers’ Mobility, Expenditure and Online-Offline Substitution Response to COVID-19: Evidence from French Transaction Data,” *European Economic Review*, 151.
- BROACH, J. P. (2016): “Travel mode choice framework incorporating realistic bike and walk routes,” Ph.D. thesis, Portland State University.
- CAILLY, C., J.-F. CÔTE, A. DAVID, J. FRIGGIT, S. GREGOIR, A. NOBRE, F. PROOST, S. SCHOFIT, N. TAUZIN, AND H. THÉLOT (2019): “Les indices Notaires-Insee des prix des logements anciens Méthodologie v4,” .
- CAROZZI, F. AND S. ROTH (2023): “Dirty density: Air quality and the density of American cities,” *Journal of Environmental Economics and Management*, 118, 102767.
- CHANDRA, A. AND E. THOMPSON (2000): “Does public infrastructure affect economic activity?: Evidence from the rural interstate highway system,” *Regional Science and Urban Economics*, 30, 457–490.
- CONLEY, T. G. (1999): “GMM estimation with cross sectional dependence,” *Journal of Econometrics*, 92, 1–45.
- CORNAGO, E., A. DIMITROPOULOS, AND W. OUESLATI (2023): “The impact of urban road pricing on the

- use of bike sharing,” *Journal of Environmental Economics and Management*, 120, 102821.
- COŞAR, A. K., B. DEMİR, D. GHOSE, AND N. YOUNG (2022): “Road capacity, domestic trade and regional outcomes,” *Journal of Economic Geography*, 22, 901–929.
- DAVIS, D. R., J. I. DINGEL, J. MONRAS, AND E. MORALES (2019): “How segregated is urban consumption?” *Journal of Political Economy*, 127, 1684–1738.
- DESHPANDE, M. AND Y. LI (2019): “Who is screened out? application costs and the targeting of disability programs,” *American Economic Journal: Economic Policy*, 11, 213–48.
- DIAMOND, R. AND E. MORETTI (2021): “Where is standard of living the highest? Local prices and the geography of consumption,” Tech. rep., National Bureau of Economic Research.
- DURANTON, G. AND M. A. TURNER (2012): “Urban growth and transportation,” *Review of Economic Studies*, 79, 1407–1440.
- GALDON-SANCHEZ, J. E., R. GIL, F. HOLUB, AND G. URIZ-UHARTE (2023): “Social Benefits and Private Costs of Driving Restriction Policies: The Impact of Madrid Central on Congestion, Pollution, and Consumer Spending,” *Journal of the European Economic Association*, 21, 1227—1267.
- GARCIA-LÓPEZ, M. A., M. MAGAGNOLI, AND E. VILADECANS (2024a): “People on bikes getting coffee. The impact of cycle lanes in cities,” *mimeo*.
- GARCIA-LÓPEZ, M. A., I. PASIDIS, AND E. VILADECANS (2024b): “Suburbanization and transportation in European cities,” *Journal of Economic Geography*, 24, 843—869.
- GIBBONS, S. AND S. MACHIN (2005): “Valuing rail access using transport innovations,” *Journal of Urban Economics*, 57, 148–169.
- GONZALEZ-NAVARRO, M. AND M. A. TURNER (2018): “Subways and urban growth: Evidence from earth,” *Journal of Urban Economics*, 108, 85–106.
- GORBACK, C. (2022): “Ridesharing and the redistribution of economic activity,” Available at SSRN 4956559.
- GROUPEMENT DES CARTES BANCAIRES (2019): “Cartes Bancaires en chiffres,” <https://www.cartes-bancaires.com/a-propos/cb-en-chiffres/>.
- HALL, J. (2021): “Can Tolling Help Everyone? Estimating the Aggregate and Distributional Consequences of Congestion Pricing,” *Journal of the European Economic Association*, 19, 441—474.
- HAMILTON, T. L. AND C. J. WICHMAN (2018): “Bicycle infrastructure and traffic congestion: Evidence from DC’s Capital Bikeshare,” *Journal of Environmental Economics and Management*, 87, 72–93.
- HEBLICH, S., S. J. REDDING, AND D. M. STURM (2020): “The making of the modern metropolis: evidence from London,” *The Quarterly Journal of Economics*, 135, 2059–2133.
- HORNBECK, R. AND M. ROTEMBERG (2024): “Growth off the rails: Aggregate productivity growth in distorted economies,” *Journal of Political Economy*, 132, 3547–3602.
- INSEE (2018): “Mobilités professionnelles en 2018 : déplacements domicile - lieu de travail Recensement de la population - Base flux de mobilité,” .
- KOSTER, H. R., I. PASIDIS, AND J. VAN OMMEREN (2019): “Shopping externalities and retail concentration: Evidence from Dutch shopping streets,” *Journal of Urban Economics*, 114, 103194.
- LANDAIS, C., D. BOUNIE, Y. CAMARA, E. FIZE, J. W. GALBRAITH, C. LAVEST, T. PAZEM, AND B. SAVATIER (2020): “Consumption Dynamics in the COVID Crisis: Real Time Insights from French Transaction & Bank Data,” CEPR Discussion Papers 15474, C.E.P.R. Discussion Papers.
- MAYER, T. AND C. TREVIEIN (2017): “The impact of urban public transportation evidence from the Paris region,” *Journal of Urban Economics*, 102, 1–21.

- McFADDEN, D. (1974): “The measurement of urban travel demand,” *Journal of Public Economics*, 3, 303–328.
- MIYAUCHI, Y., K. NAKAJIMA, AND S. J. REDDING (2021): “The economics of spatial mobility: Theory and evidence using smartphone data,” Tech. rep., National Bureau of Economic Research.
- PEREIRA, R. H. M., M. SARAIVA, D. HERSENHUT, C. K. V. BRAGA, AND M. W. CONWAY (2021): “r5r: Rapid Realistic Routing on Multimodal Transport Networks with R5 in R,” *Findings*.
- RELIHAN, L. (2022): “Is online retail killing coffee shops? estimating the winners and losers of online retail using customer transaction microdata,” .
- SCHIAVINA, M., S. FREIRE, AND K. MACMANUS (2019): “Clustering Methods: A History of k-Means Algorithms,” *GHS population grid multitemporal (1975, 1990, 2000, 2015) R2019A*.
- TASSINARI, F. (2024): “Low emission zones and traffic congestion: evidence from Madrid Central,” *Transportation Research Part A: Policy and Practice*, 185, 104099.
- THORNE, V. (2022): “Cycling Towards Cleaner Cities? Evidence from New York City’s Bike Share Program,” Tech. rep.
- TSIVANIDIS, N. (forthcoming): “Evaluating the impact of urban transit infrastructure: Evidence from bogota’s transmilenio,” *American Economic Review*.
- VIARD, V. B. AND S. FU (2015): “The effect of Beijing’s driving restrictions on pollution and economic activity,” *Journal of Public Economics*, 125, 98–115.
- WARNES, P. E. (2024): “Transport infrastructure improvements and spatial sorting: Evidence from Buenos Aires,” *Working paper*.

# Appendix

## A Additional figures and tables

Table A1: Descriptive statistics

All grid cells employed in the analysis	Mean	Std. Dev.	Min	Max
Total revenue (in 1000s €)	1,652	4,857	0	95,003
Transactions' volume	27,492	42,041	5	453,622
Avg. revenues per transaction (€)	68	126	8	2,693
Merchants (#)	28	27	1	232
Population	1,478	773	0	4,216
Population 25-39	395	248	0	1,348
Jobseekers (%)	9	2	0	19
Foreigners (%)	15	6	0	81
Cars (#)	20,782	22,714	29	166,834
House price (€per m <sup>2</sup> )	8,543	1,441	6,118	12,733
N	1,418			

Note: The percentage of job seekers is with respect to working age population, and the percentage of foreigners is with respect to the total population. All variables correspond to quarter-specific averages of the underlying monthly values (constant during the year for socioeconomic and demographic characteristics). The data are quarterly averages for 2015. Source: INSEE and *Groupement des Cartes Bancaires CB*.

Table A2: Relevance of the local bicycle length density (LBLD) control variables

	Log transaction volume		Log total revenue	
	(1)	(2)	(3)	(4)
LBLD	0.012*** (0.002)	0.005** (0.002)	0.003** (0.002)	0.006*** (0.002)
LBLD	Same project	1km	Same project	1km
Observations	27,097	27,097	27,097	27,097
R-squared	0.960	0.969	0.969	0.969
Arr-Time FE	YES	YES	YES	YES

Notes: Coefficients from the estimation of local revenue and transaction volume regressions. Robust standard errors in parentheses. \*\*\* p<0.01, \*\* p<0.05, \* p<0.1.

Table A3: Elasticity of local economic activity to market access vs. market potential

<b>Panel A:</b>		Log total revenue	
		(1)	(2)
Log MA		4.492*** (1.240)	
Log MP			14.099*** (2.942)
<b>Panel B:</b>		Log transaction volume	
Log MA		5.025*** (1.098)	
Log MP			10.019*** (3.280)
<b>Panel C:</b>		Log average revenues per transaction	
Log MA		-1.030 (0.810)	
Log MP			4.000 (2.595)
N		27,097	27,097
Controls		X	X
Grid cell FE		X	X
District×Time FE		X	X
LBDL	Same project		Same project

Notes: Coefficients from the estimation of Equation 3 in col.1; replacing market access with market potential in col.2.  $MP_{it} = \sum_{j,j \neq i} \bar{t}_{ij,t}^{-1} \text{Population}_j \times \text{Median income}_j$ . Standard errors are clustered at the district-time level. Source: *Observatoire du Plan Vélo de Paris*, INSEE and *Groupement des Cartes Bancaires CB*.

Table A4: Elasticity of local economic activity to market access: lagged impact

<b>Panel A:</b>	Log total revenue			
	(1)	(2)	(3)	(4)
Log MA	4.492*** (1.240)			
1 <sup>st</sup> lag log MA		4.180*** (1.287)		
2 <sup>nd</sup> lag log MA			3.842*** (1.393)	
3 <sup>rd</sup> lag log MA				4.868*** (1.559)
N	27,097	25,744	24,391	23,038

<b>Panel B:</b>	Log transaction volume			
Log MA	3.830*** (1.176)			
1 <sup>st</sup> lag log MA		4.676*** (1.219)		
2 <sup>nd</sup> lag log MA			4.781*** (1.355)	
3 <sup>rd</sup> lag log MA				5.951*** (1.521)
N	27,097	25,744	24,391	23,038

Notes: baseline estimation, as in column 2 of Table 1, estimating the elasticity to lagged market access. Standard errors are clustered at the district-time level. Source: *Observatoire du Plan Vélo de Paris*, INSEE and *Groupement des Cartes Bancaires CB*. Back to Section 5.1.

Table A5: Robustness tests: testing random development timing

	2017, 2 <sup>nd</sup> quarter	Treatment date 2018, 1 <sup>st</sup> quarter	2018, 4 <sup>th</sup> quarter
Log population	-3.294*** (1.028)	-0.612 (0.583)	-0.625* (0.362)
% Foreigners	16.64*** (4.818)	-1.879 (2.883)	-2.106 (1.937)
% Job seekers	-19.50** (8.822)	-17.68*** (5.196)	-0.706 (3.791)
Log population 25-39 yrs old	2.673*** (0.907)	0.561 (0.501)	0.480 (0.307)
N	271	201	146

Notes: The dependent variable is the date on which the cells in the still-to-be-developed sample as of  $s = 2017$ , 2<sup>nd</sup> quarter (col.1),  $s = 2018$ , 1<sup>st</sup> quarter (col.2) and  $s = 2018$ , 4<sup>th</sup> quarter (col.3) are going to be treated. The covariates refer to 2017, 2<sup>nd</sup> quarter (col.1), 2018, 1<sup>st</sup> quarter (col.2), 2018, 4<sup>th</sup> quarter (col.3). Back to Section 5.3.

Table A6: Robustness tests: keeping only Plan Vélo subsample

<b>Panel A:</b>		Log total revenue				
		(1)	(2)	(3)	(4)	(5)
Log MA		5.303*** (1.340)	7.058*** (1.758)	4.677*** (1.364)	5.545*** (2.03)	5.398*** (2.02)
<b>Panel B:</b>		Log transaction volume				
Log MA		8.232*** (1.642)	7.947*** (1.996)	7.641*** (1.667)	8.290*** (2.62)	8.249*** (2.61)
N		9,220	9,220	9,220	9,220	9,220
Controls		X	X	X	X	X
Grid cell FE		X	X	X	X	X
District×Time FE		X	X	X	X	X
LB LD	None	Same project		1km	-	-
Instrument					1km	Project
FS F-stat					1014.77	50493.06
Estimation			OLS			2SLS

Notes: Baseline estimation, as in Table 1 on the subsample of grid cells intersected by the original Plan Vélo. Standard errors are clustered at the district-time level. Source: *Observatoire du Plan Vélo de Paris*, INSEE and *Groupement des Cartes Bancaires CB*.

Table A7: Balancing test of local characteristics in the Plan Vélo subsample between grid cells where development had taken place by the end of 2019 and those where it did not

	Developed			Not developed			Difference	t-stat	p-value
	Mean	Std Dev	Mean	Std Dev					
MA (in 000s)	3528	970	3481	801			-47	0.57	0.57
Roads (m)	1117	342	1125	313			8	-0.25	0.80
Planned bike lanes (m)	190	109	173	89			-17	1.88	0.06
Population	1414	872	1393	751			-21	0.28	0.78
Foreigners (%)	16	5	15	4			-0	1.16	0.25
Jobseekers (%)	9	2	9	2			-0	0.73	0.47
Population 25-39	397	281	374	231			-23	0.96	0.34
Entrant firms (#)	0	1	1	1			0	-0.57	0.57
Car traffic (#)	24368	23820	19518	19703			-4850	2.38	0.02
Housing price (per m <sup>2</sup> )	8821	1635	9048	1717			227	-1.45	0.15
Total revenue (in 1000s)	1582	3060	2588	7283			1006	-1.93	0.05
Transactions' volume	30645	47632	37053	54856			6409	-1.34	0.18
Avg. value per transaction	69	152	69	69			1	-0.05	0.96
Avg. value per merchant	48504	77339	61199	127410			12695	-1.29	0.20
Merchants (#)	31	31	36	28			5	-1.75	0.08
N	229	.	232	.			.	.	.

Notes: The data are from 2015. Source: *Observatoire du Plan Vélo de Paris*, INSEE and *Groupement des Cartes Bancaires CB*. Back to Section 5.3.

Table A8: Robustness tests: elasticity of card usage intensity to market access

	Card usage intensity index			
	(1)	(2)	(3)	(4)
Log MA	0.159 (0.332)			
1 <sup>st</sup> lag log MA		0.142 (0.409)		
2 <sup>nd</sup> lag log MA			0.216 (0.470)	
3 <sup>rd</sup> lag log MA				0.312 (0.536)
N	26,948	25,604	24,260	22,916

Notes: Baseline estimation, as in Table 1 column 2 applied to the ratio between the number of establishments reporting transactions in the *Groupement des Cartes Bancaires CB* dataset in a given quarter and grid cell, and the number of establishments active in that same quarter and grid cells according to the business registry (SIRENE). Source: SIRENE, *Observatoire du Plan Vélo de Paris*, INSEE and *Groupement des Cartes Bancaires CB*. Back to Section 5.3.

Table A9: Elasticity of local economic activity to market access: testing for spatial correlation

	Log total revenue			Log transaction volume		
	(1)	(2)	(3)	(4)	(5)	(6)
Log MA	4.492*** (1.240)	4.492* (2.360)	4.492*** (1.235)	3.830*** (1.176)	3.830* (2.179)	3.830*** (1.202)
N	27,097	27,097	27,097	27,097	27,097	27,097
Controls	X	X	X	X	X	X
Grid cell FE	X	X	X	X	X	X
District×Time FE	X	X	X	X	X	X
Std Errors	Cluster District×Time	Cluster Grid cell	Conley	Cluster District×Time	Cluster District×Time	Conley Grid cell
LB LD				Same project		

Notes: Coefficients from the column 2 in Table 1 with different standard errors. Columns 1 and 4 are clustered at the district-time level. Columns 2 and 5 are clustered at the grid-cell level. Columns 3 and 6 use test 1 km spatial correlation with Conley standard errors. Source: *Observatoire du Plan Vélo de Paris*, INSEE and *Groupement des Cartes Bancaires CB*.

Table A10: Local merchant characteristics clusters: descriptive statistics

Cluster	Retail			Restaurants			Firm characteristics	
	Non spec.	Spec./food	Spec./other	Fast-food	Restaurants	Bars	Large	Old
1	30	23	10	78	8	18	18	28
2	18	63	21	90	12	65	75	63
3	6	61	89	47	19	43	74	83
4	39	28	32	1	7	8	64	80
5	29	25	64	43	60	23	71	34
All	28	35	30	56	15	27	49	52

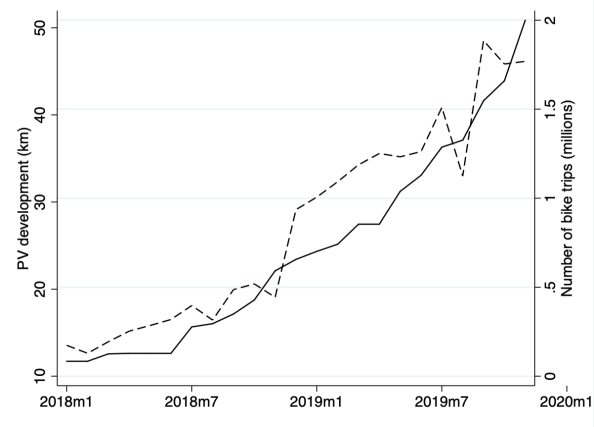
Notes: Col.1-6 contain the % of cells per cluster specialized in 2015 in the corresponding activities. Col.7-8 contain the % of cells in each cluster such that 2015 average merchant size (col.7) or age (col.8) was greater than the median value. Source: *Groupement des Cartes Bancaires CB*. Back to Section 5.4.

Table A11: Testing heterogeneous effects with respect to local merchant characteristics

	Log total revenue	Log transaction volume
Log MA $\times$ Small and new businesses	6.583*** (1.442)	4.468*** (1.196)
Log MA $\times$ Spec. food stores/fast food/bars	7.103*** (1.611)	4.965** (2.062)
Log MA $\times$ Spec. retail + old businesses	0.064 (2.343)	2.584 (1.889)
Log MA $\times$ Retail + old businesses	5.492* (3.146)	0.181 (2.787)
Log MA $\times$ Spec. retail/restaurants	-0.050 (3.020)	5.914** (2.975)
N	24,777	24,777

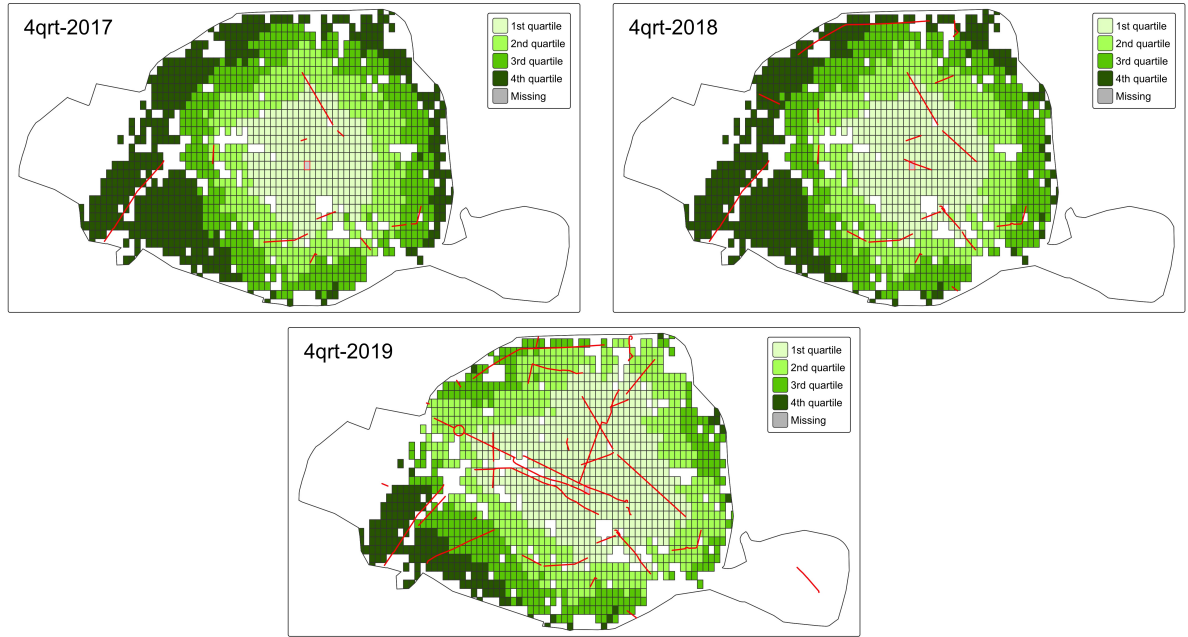
Notes: Baseline estimation, as in Table 1 column 2, testing heterogeneous effects through the inclusion of interaction terms between market access and cluster-specific dummies. The clusters were chosen through a  $k - \text{means}$  clustering algorithm and the number of clusters optimally selected through an elbow test. Source: *Observatoire du Plan Vélo de Paris*, INSEE and *Groupement des Cartes Bancaires CB*. Back to Section 5.4.

Figure A1: Total number of bicycle trips recorded in Paris over time



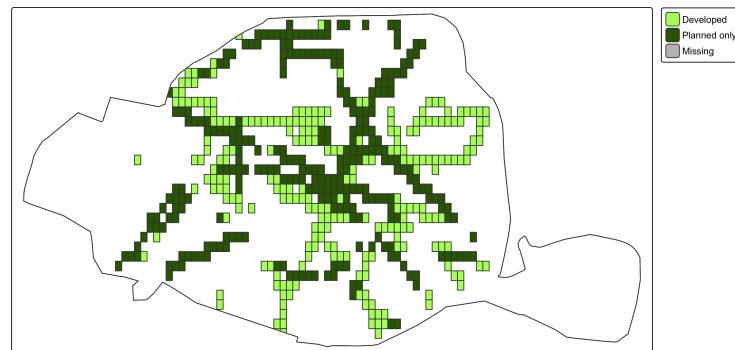
Notes: All bicycle trips were recorded using sensors distributed across the city. Source: *Comptage vélo - Données compteurs* dataset from <https://www.data.gouv.fr/en/datasets/comptage-velo-historique-donnees-compteurs-et-sites-de-comptage/>.

Figure A2: Distribution of travel times by bicycle to Hôtel de Ville at different points in time



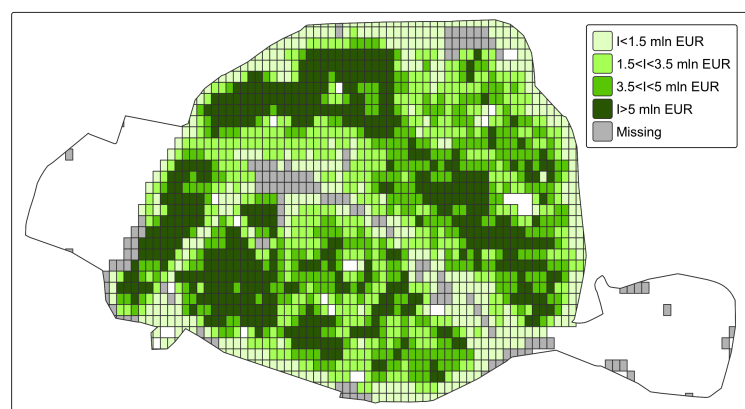
Notes: distribution of bilateral travel times by bicycle over time between Hôtel de Ville (red square) and other parts of the city. The quartiles are calculated based on the grid cell and quarter distribution and are not time-specific. First quartile: less than 21 min. commute; second quartile: between 21 and 30 min. commute; third quartile: between 30 and 39 min. commute; fourth quartile: more than 39 min. commute. The overlaid red lines show the development of Plan Vélo over time. Back to Section 3.

Figure A3: Grid cells crossed by 2015 Plan Vélo



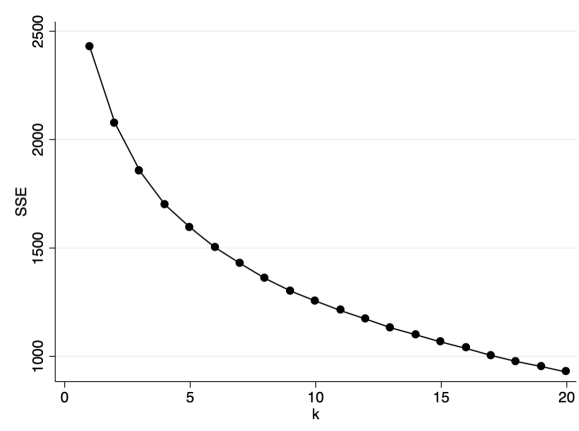
Notes: Grid cells are dark green-colored if they intersect with the actually developed Plan Vélo as of the fourth quarter of 2019; light green-colored if they intersect with the original but never developed plan.  
Source: *Observatoire du Plan Vélo de Paris*. Back to Section 5.3.

Figure A4: Spatial distribution of income



Notes: Income in a given grid cell  $j$  corresponds to  $\text{Population}_j \times \text{Median income}_j$  in 2015. Source: INSEE.  
Back to Section 5.3.

Figure A5: Elbow test for the selection of the optimal number of clusters



Notes: Sum of squared errors on the vertical axis. Back to Section [5.4](#)

## B Calculating bilateral travel times by mode

OpenStreetMap was used to estimate transport-mode-specific bilateral travel times between the centroid of each pair of grid cells forming the geographical unit of our analysis. More specifically, we combine three sources of data: i) information on the development of the *Plan Vélo* from the *Observatoire du Plan Vélo de Paris*, which tracks daily development from July 2017 through 2020 ; ii) the historical snapshot of the OpenStreetMap project (OSM) for each quarter from 2015 to 2019<sup>22</sup>; and iii) General Transit Feed Specification (GTFS) files for the city of Paris for each quarter from 2015 to 2019, provided by the Paris main public transit operator, the RATP group.<sup>23</sup>

Bilateral travel time matrices (in minutes) for public transit are obtained through the `travel_time_matrix()` function of the *Rapid Realistic Routing with R5* package for R.<sup>24</sup> This package uses Conveyal's R5 Routing Engine to calculate realistic travel times allowing it to incorporate multiple forms of public transit as well as walking within the same trip. For all public transit travel times, we fixed the departure time at 17:00 hs, or the closest time available after 17:00 h.

The construction of travel time matrices for other transport modes (walking, cycling, and driving) follows a different, more flexible approach. We begin by extracting the network of all *ways*<sup>25</sup> that is traversable by a given a mode of travel (i.e, driving, walking or cycling) from the OSM data. We then assign travel speed along each of these ways for each mode. For the driving network, we assign the speed limit (in km/h) of each street segment, according to the information on OSM for that specific moment in time. For the walking network, we assign a fixed speed of 4.5 km/h for the entire network. For speeds of the cycling network, we rely on information from OSM to classify each edge into six categories, summarized in Table A12. We assign the fastest cycling speed to cycle tracks, which are protected bike lanes that are either off-road or provide some form of physical barrier blocking car traffic.<sup>26</sup> The *Plan Vélo* provides this type of cycling infrastructure. As the new cycling infrastructure is built, information from the *Plan Vélo* is matched with the OSM network to transform the roads that overlap with the *Plan Vélo* into cycle tracks, irrespective of their status in OSM data. By doing this, we can match the timing of the new infrastructure more precisely, given

---

<sup>22</sup>Information corresponding to the first day of February, May, August, and November of every year from 2015 to 2019.

<sup>23</sup>GTFS files are an Open Standard system used to distribute relevant information about transit systems. They include all timetables for a public transit system, the location of all bus stops and metro stations, among other relevant information.

<sup>24</sup>See Pereira et al. (2021) for more details on this package.

<sup>25</sup>A way is defined as any linear feature of a map, such as a road, a sidewalk, a river, etc.

<sup>26</sup>These are equivalent to what we refer to as “bike lanes” when discussing the *Plan Vélo* infrastructure.

that OSM is a crowd-sourced project that might suffer from a small lag in updating the true conditions on the ground. For cycle tracks, we assign a cycling speed of 16 km/h. For all other categories, we adjust the speed downward by an adjustment factor that ranges from half the speed (for cycle lanes<sup>27</sup> and residential roads) to 0.17 times the speed of cycle tracks for primary, trunk and motorway roads.<sup>28</sup>

Table A12: Cycling speeds by type of edge in the cycling network

Type of edge in cycling network	Adjustment to default speed
Cycle track	1
Cycle lane	0.50
Primary, trunk or motorway	0.17
Secondary or tertiary	0.25
Unclassified one-way streets	0.50
Other (mainly residential) with no bicycle signs or infrastructure	0.50

Notes: For each highway, type as defined by the OpenStreetMap classification, we assigned a different cycling speed. The speed is calculated as a fraction of the maximum cycling speed, which is fixed at 16 km/h for cycle tracks. All other ways are adjusted by the adjustment number in this table, so, for example, the cycling speed on secondary and tertiary roads is  $16 \times 0.25 = 4$  km/h. Back to Appendix Section B.

Having derived travel speeds for each edge in each type of network (driving, cycling and walking),<sup>29</sup> we apply Dijkstra’s algorithm to find the minimum travel time between each pair of centroids, by network.<sup>30</sup> We allow travel times to be asymmetric; namely, the travel time from point A to point B can be different from the travel time from point B to point A, and repeat the calculation for every type of network (cycling, walking and driving) and quarter.

With these travel time matrices, we can define the bilateral travel time for each origin  $i$  and destination  $j$  pair, each mode  $m$ , and quarter:  $t_{ijm}$ . As the plan developed, bilateral travel times by bicycle on average decline, and more so in the proximity of the new *Plan Vélo* infrastructure.

Figure A6 illustrates how our routing algorithm captures the impact of the new bicycle infrastructure on the least-cost path for cycling. In this figure, we show the route calculated by our routing algorithm for the same trip taken by bicycle in the first quarter of 2015 (in red) and then for the last quarter of 2019 (in blue). We can see that after the *Plan Vélo* is implemented, the optimal path favors streets with bike lanes, resulting in a slightly longer

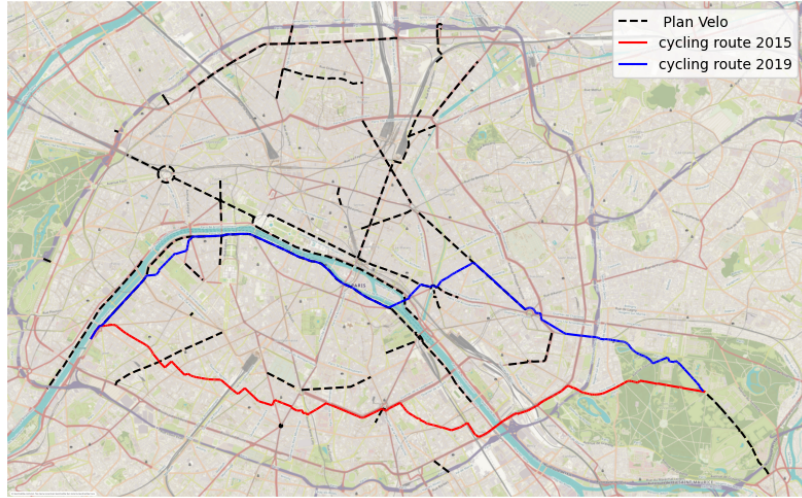
<sup>27</sup>Cycle lanes, as opposed to tracks, usually lie within the roadway itself and do not provide any physical separation with traffic. They are usually marked with painted lines and signs on the pavement and may be shared with buses.

<sup>28</sup>These adjustments to the cycling speed follow a similar logic to Broach (2016), which provides generalized cost formulas for cycling, where the cost of cycling depends on the type of infrastructure and the density of traffic, among other factors.

<sup>29</sup>An edge in these networks is defined as an ordered pair of nodes, and a node is created every time two *ways* intersect. Within a city, most of these edges coincide with the intuitive notion of a city block.

<sup>30</sup>To do so, we treat the network as a directed graph, where the weights for each edge are defined by the time it takes to traverse said edge. Technically, we match the centroid to the closest node on the graph, so the travel times are to the closest nodes on the graph to the centroids of each cell.

Figure A6: Example of cycling route before and after *Plan Vélo*



Notes: Example of the least-cost path for cycling calculated by our routing algorithm for the first quarter of 2015 (before the *Plan Vélo*), in red, and for the last quarter of 2019 (after the *Plan Vélo*), in blue. The trip in 2015 was estimated to take 114 minutes, while the trip in 2019 would take 92 minutes, implying a 20% reduction in travel time. Back to Appendix Section B.

trip (measured in distance), but that is 20% faster (going from 114 minutes in 2015 to 92 minutes in 2019).

In Figure A7, we compare the travel times by bicycle estimated by Google Maps on June 2024 for a set of 8,000 random origin-destination pairs to the travel times for these same trips estimated by our routing algorithm in the last quarter of 2019. We can see that our estimates are highly correlated with those produced by Google Maps. A linear regression of our estimates on the Google Maps travel times produces a coefficient of 0.61 (significant at a 1% level), and an intercept of 1.2 minutes. This suggests that our travel time estimates are largely proportional to those estimated by Google Maps.

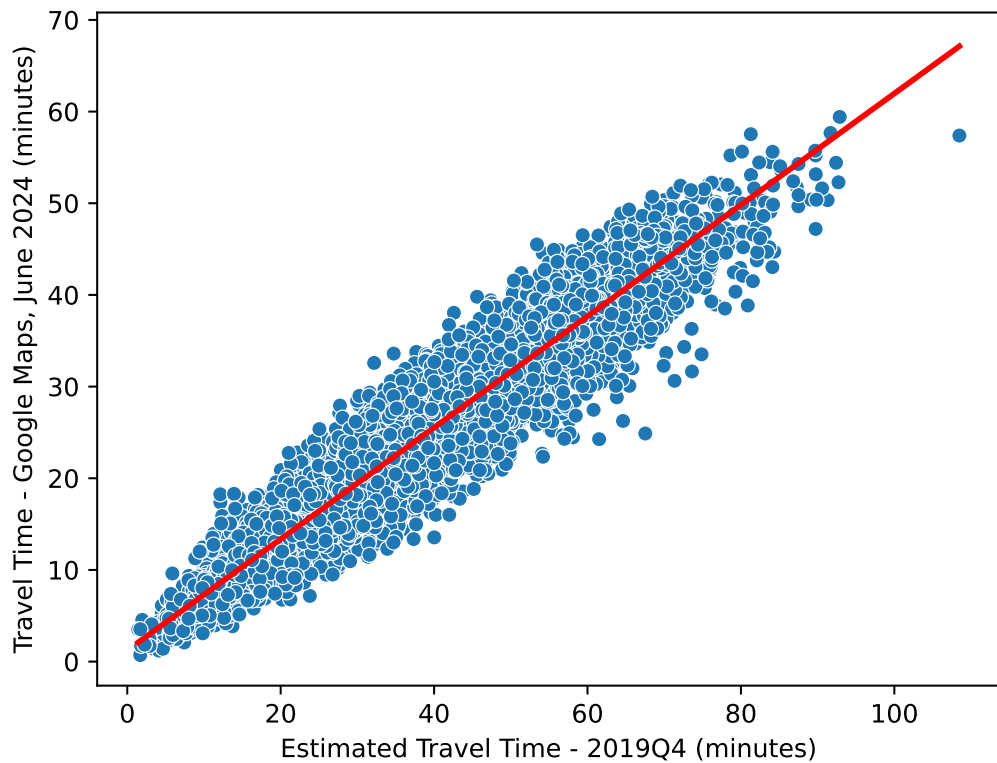
## C Microfounding the link between brick-and-mortar consumption and market access

The link between brick-and-mortar consumption and market access is demonstrated by means of a simple partial equilibrium model, where consumers choose the location to consume, as well as the mode of transport they will use to travel to that location.<sup>31</sup> A resident of location  $j$  maximizes a Cobb-Douglas utility by choosing how much to consume of a housing good ( $h_j$ ), a durable good (also the numeraire,  $d_j$ ), and a non-durable ( $nd_j^i$ ) good, and in which location  $i$  to purchase the latter:

---

<sup>31</sup>The shopping and modal choice problems are similar to Gorback (2022) and Tsivanidis (forthcoming).

Figure A7: Bilateral travel times by bicycle: Google Maps vs own estimates



Notes: Comparison between bilateral travel times estimated by Google Maps on June 2024 for cycling trips in Paris and the travel time estimates for those same origin-destination pairs for the fourth quarter of 2019 using our routing algorithm. 8,000 origin-destination pairs were chosen at random from the set of all trips from the centroid of one cell to the centroid of another cell in Paris. We then queried these trips on Google Maps and compared the estimated travel times to those produced by our routing algorithm for the fourth quarter of 2019. The red line represents a linear fit of the data, with a coefficient of 0.61 and an intercept of 1.2 minutes. The R-squared of this regression is 0.9. Back to Appendix Section [B](#).

$$\max_{h_j, d_j, nd_j^i} \left( \frac{h_j}{\beta} \right)^\beta \left( \frac{d_j}{\alpha} \right)^\alpha \left( \frac{nd_j^i}{1 - \alpha - \beta} \right)^{1-\alpha-\beta} \frac{z_{ij}}{dis_{ij}} \quad s.t. \quad I_j = q^j h_j + d_j + p^i nd_j^i \quad (6)$$

where  $I_j$  is the income of residents of location  $j$ ,  $q^j$  is the price for the housing good in location  $j$  and  $p^i$  is the price for the non-durable good sold in location  $i$ .  $\beta$  and  $\alpha$  are the housing and durable good shares, respectively. The choice of where to purchase the non-durable good depends on a bilateral idiosyncratic preference shock,  $z_{ij}$ , which is Fréchet distributed  $F(z_{ij} = \exp(-E_i z_{ij}^{-\varepsilon}))$ , where  $E_i$  is a destination-level amenity parameter and  $\varepsilon$  governs the substitutability between consumption locations. This choice also depends on the disutility of travel from home  $j$  to the shopping destination  $i$ ,  $dis_{ij}$ .

Consumers can choose to commute via a private transport mode (conditionally on owning a car, which happens with probability  $\rho$ ),  $\mathcal{M}_{Private} = \{\text{Car}\}$ , or via a public transport mode,  $\mathcal{M}_{Public} = \{\text{Walking, Public Transport, Cycling}\}$ . The disutility of traveling via transport mode  $m \in \{\mathcal{M}_{Private} \cup \mathcal{M}_{Public}\}$  is given by  $dis_{ijm} = \exp(\kappa t_{ijm} - b_m + v_{ijm})$ , where  $t_{ijm}$  is the bilateral cost, expressed in terms of the time (in minutes) that it takes to go from  $j$  to  $i$  via transport mode  $m$ ,  $\kappa$  is the disutility of travel elasticity to transport costs,  $b_m$  is a mode-specific common preference shifter, and  $v_{ijm}$  is a second (this time mode-specific) bilateral idiosyncratic preference shock, distributed according to a Generalized Extreme Value (GEV) allowing for a nested logit estimation of the parameters governing the modal choice problem (McFadden, 1974):

$$F(\mathbf{v}) = 1 - \exp \left( - \sum_k \left( \sum_{m \in \mathcal{M}_k} \exp((v_{ijm} - b_m)/\lambda_k) \right)^{\lambda_k} \right) \quad k \in \{\text{Private, Public}\}$$

The parameter  $\lambda_{Public}$ , or simply  $\lambda$  since  $\lambda_{Private} = 1$  by construction, allows for correlation within the public transport modes nest, with the correlation increasing as  $\lambda \rightarrow 0$ .

The consumer problem is solved by backward induction. Since consumers choose first where to go shopping and next how to get there, the first choice problem to be solved is the modal choice one. Expected disutility of traveling from  $j$  to  $i$  before the realization of the mode-specific idiosyncratic preference shocks is  $dis_{ij} = \exp(\kappa \bar{t}_{ij})$ , where  $\bar{t}_{ij}$  is a weighted average of the bilateral travel cost across transport modes, with weights depending on the share of commuters choosing a given transport mode based on their car ownership status. Specifically:

$$\begin{aligned}
\bar{t}_{ij} &= -\frac{1}{\kappa} \ln [(1-\rho) \exp(-\kappa t_{ij, NoCarOwner}) + \rho \exp(-\kappa t_{ij, CarOwner})] \\
t_{ij, NoCarOwner} &= -\frac{\lambda}{\kappa} \ln \left( \sum_{k \in \mathcal{M}_k} \exp \left( \frac{b_k - \kappa t_{ij,k}}{\lambda} \right) \right) \\
t_{ij, CarOwner} &= -\frac{1}{\kappa} \ln (\exp(b_{car} - \kappa t_{ij, car}) + \exp(-\kappa t_{ij, 0}))
\end{aligned} \tag{7}$$

With the expected disutility of traveling at hand, we then move backwards to the solution of the shopping location problem. The probability of purchasing the non-durable good in location  $i$  is  $Pr_{ij} = \frac{E_i \exp(-\nu \bar{t}_{ij})}{\sum_s E_s \exp(-\nu \bar{t}_{sj})}$ , which is decreasing in the bilateral expected travel costs,  $\bar{t}_{ij}$ . The parameter  $\nu = \varepsilon \kappa$  identifies the semi-elasticity of consumption-related travel flows to travel costs and it is a combination of the disutility of travel elasticity parameter,  $\kappa$ , and the travel heterogeneity parameter,  $\varepsilon$ .

In a context where  $\bar{t}_{ij}$  declines on average for all origin and destination pairs because of the development of new transport infrastructure, a shopping location  $i$  experiences an increase in market access only if the expected travel costs decline more than elsewhere. Importantly, a generalized decline in  $\bar{t}_{ij}$  does not entail an increase in aggregate expenditure, but rather a shift of expenditure towards locations that become easier to reach in relative terms since by construction consumers can shop in one location only.

The market accessible by firm in location  $i$  can then be derived by combining the just discussed probabilities and the solution to the standard Cobb-Douglas utility maximization problem:

$$MA_i = (1 - \alpha - \beta) \sum_j \frac{E_i \exp(-\nu \bar{t}_{ij})}{\sum_s E_s \exp(-\nu \bar{t}_{sj})} \times R_j \times I_j \tag{8}$$

where  $R_j$  is the measure of consumers residing in  $j$  and  $(1 - \alpha - \beta)$  the fraction of income that they spend on the non-durable good.

## D Deriving an empirical market access proxy

We derive an empirical proxy for market access in Equation 8 by combining observed bilateral travel times with the parameters of the modal choice problem estimated via a nested logit specification run on commuting flow data from the 2018 census ([INSEE, 2018](#)). The estimated parameters are used to construct bilateral expected travel costs,  $\bar{t}_{ij}$ , and retrieve, together with a subsample of bilateral consumption flow data, the semi-elasticity of bilateral consumption flows to travel costs,  $\nu$ . Below, we provide a more detailed descriptions of the

steps taken.

**Step 1: nested logit estimation** — The observed bilateral travel costs are converted into disutilities (Equation 6),  $dis_{ij}$ , through a modal choice nested logit estimation based on the commuting module of the 2018 Census (INSEE, 2018). We retain full-time workers residing and commuting within the city of Paris, for a total of 163.000 trips with non-missing information on the transport mode chosen to commute to work. Information on the place of residence/work in the survey is available at the district level, for a total of 20 districts, or *arrondissements*. The 2230-by-2230 commuting cost matrices are then aggregated into 20-by-20 matrices to match them with the information contained in the commuting survey. We choose simple bilateral averages, but test the robustness of the estimates to alternative aggregation routines.

The output of the nested logit estimation is displayed in Table A13. We estimate a disutility of travel elasticity  $\kappa = 0.003$ : an increase in travel time via a specific transport mode by 10 minutes translates into a 3 percentage points lower probability of choosing to commute via that mode compared to walking (the base category). This elasticity is three times smaller than in Tsivanidis (forthcoming).<sup>32</sup> The smaller size of the municipality of Paris compared to Bogotá could explain the discrepancy: shorter distances reduce consumers' responsiveness to differences in travel times across transport modes. The inverse of correlation across mode-specific idiosyncratic preference shocks is 0.041, denoting a sizable correlation across idiosyncratic mode-specific preference shocks. Both the cycling and car-specific common preference shifters are negative, implying a preference by consumers for walking between two destinations holding travel time constant, as opposed to cycling or driving. Conversely, the common preference shifter for public transport is positive, denoting a preference for public transport compared to walking, once again assuming identical travel times.

The estimated parameters are combined with information on the car ownership rate in the city of Paris  $\rho = 0.37$  to obtain an estimate of expected bilateral travel costs  $\bar{t}_{ij}$  according to Equation 7.<sup>33</sup>

**Step 2: estimating the semi-elasticity of consumption-related travel flows to travel costs** — Plugging the estimated expected bilateral travel costs,  $\bar{t}_{ij}$ , into the shopping location choice problem, the probability of purchasing the non-tradable good in location

---

<sup>32</sup>Recent work by Miyauchi et al. (2021) finds the commuting elasticity estimated based on consumption-related trips to be higher than the one based on work-related trips.

<sup>33</sup>A normalization is implemented to ensure that  $\bar{t}_{ii} = 0$ . More specifically,  $t_{ij,0}$  is rescaled by  $-(\lambda/\kappa) \ln(\exp(b_{walking}/\lambda) + \exp(b_{cycling}/\lambda) + \exp(b_{pt}/\lambda))$  and  $t_{ij,1}$  is rescaled by  $-(1/\kappa) \ln(\exp(b_{car}) + 1)$ .

Table A13: Estimated modal choice parameters

Description	Parameter	Value
Disutility of travel elasticity to travel time	$\kappa$	.003
Inverse of correlation across mode-specific idiosyncratic preference shocks	$\lambda$	.041
Cycling preference shifter	$b_{cycling}$	-.065
Public transport preference shifter	$b_{pt}$	.029
Car preference shifter	$b_{car}$	-2.76

Note: The conditional logit estimation is implemented using the `nlogit` STATA module. The base category is walking. Back to Section 3.

$i$  is:

$$Pr_{ij} = \frac{E_i \exp(-\nu \bar{t}_{ij})}{\sum_s E_s \exp(-\nu \bar{t}_{sj})} \quad (9)$$

where  $\nu$  identifies the semi-elasticity of bilateral consumption flows to travel costs.

To build an empirical counterpart of the market access measure described in Equation 8, an estimate of  $\nu$  is required. However, bilateral travel flows are not directly observed in our dataset. Hence, we developed an imputation procedure to calculate a proxy for them using data from 2019. Specifically, we observe daily transactions indexed by the merchant and card identifier. We do not know where the cardholder lives, nor do we have any demographic information on him/her. However, we can impute a “most likely” residence location based on each cardholder’s shopping history.

1. First, we retain transactions occurring in the city of Paris on weekends and weekdays after 18h;
2. Second, we retain transactions that are usually carried out in the proximity of one’s residence, which we identify as transactions occurring in merchants identified by one of the following sectoral codes: 1071, 1072, 4724 (bakeries), 4773 (pharmacies), 4711B-D (supermarkets, minimarkets), 4721, 4722, 4723, 4725, and 4729 (food stores).
3. Next, we keep cardholders for which the number of observed transactions is  $N \geq 9$ .

We end up with a sample of 3.2 million cards, about  $1/8^{th}$  of the total number of cards present in the data, but amounting to nearly half (49%) of the transactions’ total value. For this subset of cards, we calculate the modal shopping destination and we set it as “most likely” residence location,  $j$ . Bilateral travel flows,  $x_{ij}$ , are calculated by summing across transactions carried out by cardholders with imputed residence location  $j$  towards merchants

with (known) business location  $i$ , and are used to estimate the empirical counterpart of Equation 9:

$$\ln x_{ij} = \alpha_i + \alpha_j + \nu \bar{t}_{ij} + e_{ij} \quad (10)$$

In Equation 10, the  $\bar{t}_{ij}$  are the estimated expected bilateral travel costs obtained in the previous step and  $\alpha_i$  and  $\alpha_j$  are business and residence location fixed effects, respectively. The estimation is repeated for four different quarters of 2018. We consistently estimate  $\hat{\nu} = 0.1$ , similar to the 0.07 estimated by Ahlfeldt et al. (2015).

Finally, we use the estimated  $\bar{t}_{ij} \forall i, j$  and  $\hat{\nu}$  to derive an empirical proxy for market access in Equation 8:

$$\text{MarketAccess}_{it} = \sum_{ij} \frac{\exp(-\hat{\nu} \bar{t}_{ij,t})}{\sum_s \exp(-\hat{\nu} \bar{t}_{sj,t})} \times \text{Population}_j \times \text{Median income}_j$$

When taking Equation 8 to the data, we implement a few simplifications. First, we fix the population, median income, and travel times by modes other than cycling to their levels measured in the first quarter of 2015. By doing so, we allow our empirical market access proxy to only vary through two channels: the direct channel of changes in the travel times by bicycle, and the indirect channel of changes in the adoption of cycling as a consequence of the new travel times through the modal choice problem.<sup>34</sup> The empirical market access proxy will then differ from the theoretical measure in Equation 8. Because of this, we would not expect the coefficient associated with regressing total revenue on this measure to be exactly 1, since this regression will capture how much of the variation in total demand in each location in Paris in this period can be attributed to changes in cycling travel times and its impact on the modal choice of consumers.

## 7 Additional Robustness Tests

**Household sorting** — Evidence has shown that investment in infrastructure can impact household sorting Tsivanidis (forthcoming). If this is the case, it could be that part of the effect of an improvement in market access on business revenues is due to a different

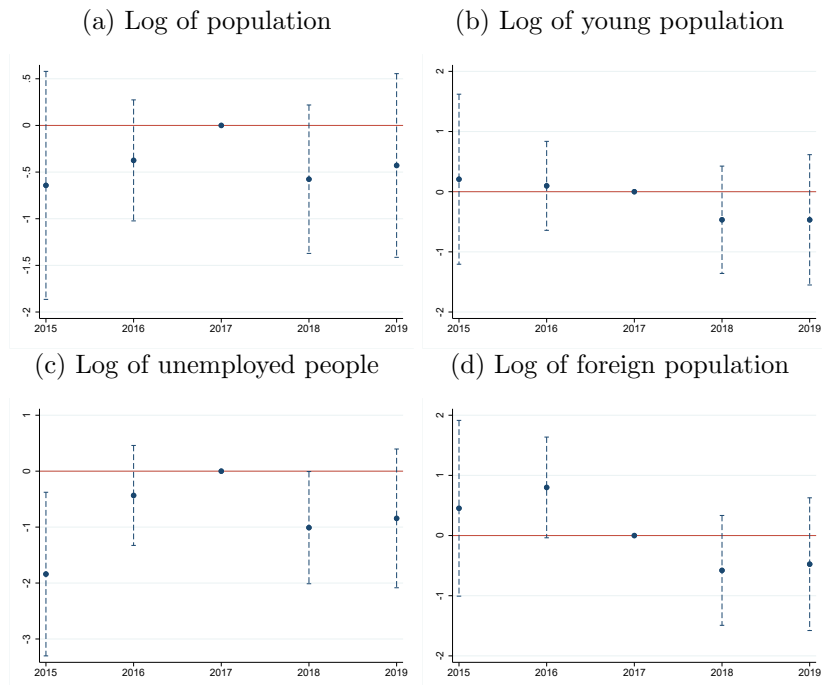
---

<sup>34</sup>As bicycle travel costs go down two things happen: 1) the unweighted average travel cost to go from  $j$  to  $i$  drops, and 2) the share of consumers choosing to go shopping by bicycle increases, thus magnifying the impact of the reduction in bicycle travel costs on the bilateral disutility of traveling (which also drops). While the number of consumers going shopping from  $j$  to  $i$  by bicycle unambiguously rises, the number of consumers choosing to drive might decline if the negative impact on the car modal share outweighs the expected increase in the number of consumers living in  $j$  choosing to go shopping in  $i$ . The chosen setup thus allows to account for substitution across transport modes.

composition of local residents rather than the development of bike lane infrastructure. For instance, the development of bike lanes might have triggered the inflow of young people, who tend to go out and consume more in bars and restaurants.

In our baseline specification, we control for (a three-year lag of) local demographic characteristics to address the potential effect of changing local residents' composition. Alternatively, we can investigate how neighborhoods with different levels of market access changed during the five years of the analysis. We do so by running the pre-trends analysis as in Equation 4, using the available demographic controls as outcome variables.<sup>35</sup> Results reported in Figure A8 show that places that experienced greater market access improvements by the end of the study period did not experience any statistically significant variation in demographic composition. This evidence is consistent with household sorting being a process occurring in the medium-run, in contrast to the short-run focus of our analysis.

Figure A8: Household sorting: changes in demographic characteristics



Notes: Estimated  $\beta^t$  from Equation 4 on the y-axis. Source: *Observatoire du Plan Vélo de Paris*, INSEE and *Groupement des Cartes Bancaires CB*.

**Other potentially confounding factors —** In Table A14, we present a set of further robustness tests. In column 2, we control for lagged sectoral shares to ensure that our

<sup>35</sup>We remove the controls  $X_{i,t}$  for the purpose of this test. Due to data availability, this test is performed annually instead of quarterly.

results are not driven by changes in the composition of local economic activity.<sup>36</sup> Second, in columns 3 and 4, we test the robustness of our results to a law passed in 2015 that allowed businesses located in certain parts of the city to stay open on Sundays. A map of the places of concern is shown in Figure A9. Data were obtained from APUR, *Mairie de Paris* and DRIEA IF/UD75. Since our card transaction dataset is available at the monthly frequency, we cannot exclude transactions carried out on Sundays and directly control for potentially endogenous self-selection into this policy. Instead, we remove grid cells that were affected by the Sunday Law (column 3), or, alternatively, we include an interaction term between the grid cell-specific share of surface concerned by the law and time dummies (column 4). Across all tests, the elasticity of total revenue and transaction volume to market access remains positive and statistically significant.

Figure A9: Places concerned by the Sunday Law



Notes: Dark green zones include international tourism areas, tourism areas, commercial areas and train stations. Source: APUR, *Mairie de Paris* and DRIEA IF/UD75.

---

<sup>36</sup>Specifically, we include the lagged share of revenues for each grid cell and time in the following non-durable sub-sectors: non-specialized retail stores (Code NAF 471), specialized food retail stores (Code NAF 472), specialized non-food retail stores (Code NAF 474-477), fast food restaurants and bars (Code NAF 561), restaurants (Code NAF 562), bars specialized in the sale of drinks (Code NAF 563).

Table A14: Robustness tests: miscellanea

<b>Panel A:</b>		Log total revenue			
		(1)	(2)	(3)	(4)
Log MA		4.492*** (1.240)	3.627*** (1.218)	6.292*** (1.221)	4.533*** (1.204)
<b>Panel B:</b>		Log transaction volume			
Log MA		3.830*** (1.175)	3.388*** (1.182)	4.855*** (1.180)	3.883*** (1.135)
N		27,097	25,740	22,157	27,097
Test		Baseline	Sectoral shares	Remove affected by Sunday Law	Sunday Law trend

Notes: baseline estimation, as in Table 1 column 2 (col.1); augmented to include lagged sectoral shares as controls (col.2); excluding cells affected by the Sunday Law (col.3); augmented to include an interaction term between the grid cell-specific share of surface concerned by the 2015 “Sunday Law” and time dummies (col.4); excluding grid cells located within 100 meters from the itinerary of tramway T3b (col.5); . Standard errors are clustered at the grid cell level. Source: *Observatoire du Plan Vélo de Paris*, INSEE and *Groupement des Cartes Bancaires CB*.